Mg/Ca-temperature calibration for the benthic foraminifera *Melonis barleeanum* and *Melonis pompilioides*

Adam P. Hasenfratz[1,2*], Ralf Schiebel[3], David J. R. Thornalley[4], Joachim Schönfeld[5], Samuel L. Jaccard[2], Alfredo Martínez-García[3], Ann Holbourn[6], Anne E. Jennings[7], Wolfgang Kuhnt[6], Caroline H. Lear[8], Thomas M. Marchitto[7], Ursula Quillmann[7], Yair Rosenthal[9], Jimin Yu[10], Gerald H. Haug[1,3]

[1]Geological Institute, Department of Earth Sciences, ETH Zurich, Zurich, Switzerland

[2]Institute of Geological Sciences and Oeschger Centre for Climate Change Research, University of Bern, Bern, Switzerland

[3]Max Planck Institute for Chemistry, Mainz, Germany

[4]Department of Geography, University College London, London, UK

[5]GEOMAR – Helmholtz-Centre for Ocean Research Kiel, Kiel, Germany

[6]Institute of Geosciences, Christian-Albrechts-University, Kiel, Germany

[7]Department of Geological Sciences and Institute of Arctic and Alpine Research, University of Colorado, Boulder CO, USA

[8]School of Earth and Ocean Sciences, Cardiff University, Cardiff, UK

[9]Department of Marine and Coastal Sciences, Rutgers University, New Brunswick NJ, USA, and Department of Earth and Planetary Sciences, Rutgers University, Piscataway NJ, USA

[10]Research School of Earth Sciences, The Australian National University, Canberra, Australia

* Corresponding author.

E-Mail address: adam.hasenfratz@geo.unibe.ch (A. P. Hasenfratz).

Abstract

An important tool for deep-sea temperature reconstruction is Mg/Ca paleothermometry applied to benthic foraminifera. Foraminifera of the genus *Melonis* appear to be promising candidates for temperature reconstructions due to their wide geographical and bathymetric distribution, and their infaunal habitat, which was suggested to reduce secondary effects from carbonate ion saturation ($\Delta[CO_3^{2-}]$). Here, we make substantial advances to previous calibration efforts and present new multi-lab Mg/Ca data for *Melonis barleeanum* and *Melonis pompilioides* from more than one hundred core top samples spanning *in situ* bottom temperatures from −1 to 16°C, coupled with morphometric analyses of the foraminifer tests. Both species and their morphotypes seem to have a similar response of Mg/Ca to growth temperature. Compilation of new and previously published data reveals a linear dependence of temperature on Mg/Ca, with a best fit of Mg/Ca (mmol/mol) = 0.113 ± 0.005 * *BWT* (°C) + 0.792 ± 0.036 (r^2 = 0.81; n=120; 1σ SD). Salinity, bottom water $\Delta[CO_3^{2-}]$, and varying morphotypes have no apparent effect on the Mg/Ca-temperature relationship, but pore water $\Delta[CO_3^{2-}]$ might have had an influence on some of the samples from the tropical Atlantic.

1. INTRODUCTION

Subsurface temperature reconstructions in the high latitudes are critical to an assessment of changes in paleocirculation, density stratification, and ice volume, with high latitude regions such as the Nordic Seas and the Southern Ocean being of particular importance (e.g., Elderfield et al., 2012, Ezat et al., 2014, Roberts et al., 2016). The oxygen isotopic composition of benthic foraminifer tests ($\delta^{18}O_C$) is often used in high-latitude paleoceanography (e.g., Dokken and Jansen, 1999; Bach and Bauch, 2001; Waelbroeck et al., 2002; Meland et al., 2008; Thornalley et al., 2010), but its interpretation is hindered by the multiple influences on $\delta^{18}O_C$. Mg/Ca paleothermometry applied on benthic foraminifera can be used to constrain calcification temperatures owing to the temperature-dependent

partitioning of Mg during calcification (Nürnberg et al., 1996; Rosenthal et al., 1997). Many Mg/Ca-temperature calibrations have been conducted on epifaunal *Cibicidoides* species (e.g., Lear et al., 2002; Marchitto et al., 2007; Lo Giudice Capelli et al., 2015), but the sensitivity of epifaunal Mg/Ca to temperature has recently been questioned for low temperatures (typical of high-latitudes and the deep ocean) due to the carbonate ion saturation ($\Delta[CO_3^{2-}]$) effect (Elderfield et al., 2006; Yu and Elderfield, 2008). As pore water $[CO_3^{2-}]$ has been shown to equilibrate with $CaCO_3$ at shallow depths within the sediment (Martin and Sayles, 1996; 2006), it has been suggested that infaunal benthic foraminifera calcifying in the surface sediment would be expected to show a weaker relationship with $\Delta[CO_3^{2-}]$ than epifaunal species (Elderfield et al., 2006; 2010). In the paleoceanographically important high-latitude regions, species of the cosmopolitan genus *Melonis* are often one of the dominant infaunal foraminifera, such as in the Nordic Seas (Belanger and Streeter, 1980; Mackensen et al., 1985), the northern North Atlantic (Thornalley et al., 2010), and the Southern Ocean (Mackensen et al., 1993; Mackensen et al., 1995).

The two existing, independent *Melonis* Mg/Ca-temperature calibrations suffer from significant uncertainties in their robustness and fidelity. The calibration of Lear et al. (2002) (0.8−18.4°C) is primarily based on samples from the Little Bahama Bank (LBB) that are very likely affected by high-Mg calcite overgrowth (e.g., Marchitto et al., 2007; Regenberg et al., 2007; Curry and Marchitto, 2008), whereas the Kristjansdottir et al. (2007) calibration (−0.2−7.0°C) is limited to core top samples retrieved from the shallow Iceland Shelf and a single sample from the Greenland margin, where seasonal and annual temperature fluctuations can amount to more than 5°C (Malmberg and Jonsson, 1997; Kristjansdottir et al., 2007), increasing uncertainty in the calcification temperature that should be used for calibration. Here, we present new multi-lab Mg/Ca data for *M. barleeanum* and *M. pompilioides* based on more than one hundred core top samples that span a wide geographic area, including bottom water temperatures from −0.9°C to 15.6°C. We evaluate the effect of salinity, bottom water $\Delta[CO_3^{2-}]$ and different morphotypes on the Mg/Ca values of *Melonis*

75 spp. We finally propose a new Mg/Ca-temperature calibration based on the new data as well
76 as published data.

77 2. MATERIALS AND METHODS

78 2.1 Taxonomy and depth habitat of *Melonis*

79 The discrimination of extant *Melonis* species is mainly based on the spiral height of the test
80 and the number of chambers per whorl. Due to intraspecific variability in test morphology
81 including regional differences, probably caused by ecophenotypes, the identification of
82 different *Melonis* species is not unequivocal (Boltovskoy, 1958; Berggren et al., 1976;
83 Wright, 1978; Corliss, 1979; Mead, 1985; van Morkhoven et al., 1986; Thies, 1991;
84 Mackensen et al., 1993; Bergamin et al., 1997; Milker and Schmiedl, 2012; Holbourn et al.,
85 2013). Several *Melonis* species are considered as cospecific to the two most widely used
86 species *M. barleeanum* (or *M. barleeanus*) and *M. pompilioides* (e.g., Boltovskoy, 1958; van
87 Morkhoven et al., 1986) (Fig. 1). The rather compressed test of *M. barleeanum* (Williamson
88 1858) has approximately 10−12 moderately inflated chambers that gradually increase in size
89 (Holbourn et al., 2013). *Melonis zaandami* (Voorthuysen 1952) is considered as younger
90 synonym of *M. barleeanum* (Lutze et al., 1979; van Morkhoven, 1986; Thies, 1991; Schiebel,
91 1992; Mackensen et al., 1993; Jones, 1994; Altenbach et al., 1999). The name *M. affinis*
92 (Reuss 1851) should be used for Paleogene species only, because their type level is Oligocene
93 (Holbourn et al., 2013). The more spherical test of *M. pompilioides* (Fichtel and Moll 1798)
94 has approximately 8−12 chambers that are strongly inflated and increase considerably in size
95 and width during ontogeny (Holbourn et al., 2013). The deep-water form *M. sphaeroides*
96 (Voloshinova 1958) is morphologically very similar to *M. pompilioides* and, by some authors,
97 is considered an ecophenotype of *M. pompilioides* rather than a distinct species (van
98 Morkhoven et al., 1986; Jones, 1994; Berggren and Kaminski, 1990; Holbourn et al., 2013).
99 Furthermore, *M. soldanii* (d'Orbigny 1846) and *M. parkerae* (Uchio 1960) are considered as
100 junior synonyms of *M. pompilioides* (Boltovskoy, 1958; Berggren et al., 1976; Mead, 1985;
101 van Morkhoven et al., 1986). The depth distribution of infaunal *M. barleeanum* is affected by

oxygen availability, redox boundaries, and food sources, and is largely limited to the upper 3 cm within the mesobathyal ocean floor (e.g., Jorissen et al. 1998; Fontanier et al., 2002; 2006; Schmiedl and Mackensen, 2006), although they can be occasionally found deeper in the sediment (Schumacher, 2001). Furthermore, the species is known to migrate to the sediment surface during times of low food availability (Linke and Lutze, 1993; Schönfeld, 2001). There are not many studies on the depth distribution of the usually less abundant *M. pompilioides* that was found to prefer an infaunal depth habitat closer to the surface (~0−1 cm) in the South Atlantic (Schumacher, 2001).

2.2 Sampling strategy

This work focuses on samples from several independent studies. A first group of 95 surface samples, curated at the Institute of Geosciences, University of Kiel, was collected from the Eastern North Atlantic Ocean on various cruises within the framework of the North to South Atlantic Ocean Foraminiferal Transects (NOSOFO) project (Table 1, Fig. 2). The selection of the NOSOFO surface sediment samples for this study was based on previous work on living benthic foraminiferal assemblages (Seiler, 1975; Haake, 1980; Lutze and Coulbourn, 1984; Mackensen et al., 1985; Thies, 1991; Timm, 1992; Schiebel, 1992; Altenbach et al., 1999; Altenbach et al., 2003; Schönfeld and Altenbach, 2005). *Melonis* specimens from these samples, together with one Pacific Southern Ocean core top, were morphometrically analyzed at the Department of Climate Geochemistry, Max Planck Institute for Chemistry (MPIC), and their geochemical composition was measured at the Geological Institute, ETH Zurich (ETHZ). A second supplementary set of core top samples from high sedimentation rate cores in the subpolar North Atlantic were utilized, with samples from 11 core sites cleaned and measured at the School of Earth and Ocean Sciences, Cardiff University (CU), samples from a further two core sites analyzed at the Godwin Laboratory for Palaeoclimatic Research, Department of Earth Sciences, University of Cambridge (GLPR), and one surface sediment sample analyzed at the Institute of Arctic and Alpine Research, University of Colorado (INSTAAR). Another five core tops were retrieved from the Oslofjord (Risdal, 1964) and also

129 processed at INSTAAR. Three additional samples were obtained from the Sulawesi margins
130 in Indonesia and analyzed at CU. Finally, one core top sample from the eastern South Atlantic
131 was processed at the Department of Earth Sciences, University of Bristol (UoB). Overall, the
132 core top sediments span a wide latitudinal range from the tropics to polar realms and were
133 retrieved from water depths ranging between 50 and 4305 m (Table 1, Fig. 2).

134 **2.3 Analytical techniques at MPIC and ETHZ**

135 Depending on the abundance of *Melonis* (Table 1), a varying number of dead individuals (13
136 ± 6 individuals, 255 ± 127 µg) was picked from the >250 µm size range at the Institute of
137 Geosciences, University of Kiel. In order to allow a clear distinction between the compressed
138 *M. barleeanum* and the inflated *M. pompilioides*, morphometric analyses of the foraminifer
139 tests were carried out at MPIC. Tests were photographed using an Olympus SZX16 binocular
140 incident light microscope with a planapochromatic objective, equipped with an Olympus
141 UC90 digital camera (image resolution of 1.32 x 1.32 µm per pixel). All individuals were
142 photographed from the side in order to allow counting of chambers. Well-preserved
143 representatives of compressed to spherical morphotypes from all samples, i.e. a total of 452
144 tests, were photographed in frontal view in order to determine the aspect ratio (AR). The AR
145 of the foraminifer test denotes the ratio between spiral height (maximum test diameter) and
146 spiral width (maximum test diameter perpendicular to the plane of symmetry of the
147 planispiral tests) (see Fig. 3a), and was determined in an automated way using the image
148 analysis software Olympus Stream Essentials version 2.1.

149 Following the morphometric analyses, samples were cleaned and analyzed for trace metals at
150 ETHZ. The cleaning procedure applied is that published by Barker et al. (2003), i.e. omitting
151 the reductive cleaning step (Boyle and Keigwin, 1985) that has been shown to lower the
152 Mg/Ca ratio of the remaining biogenic carbonate (Martin and Lea, 2002; Barker et al., 2003;
153 Rosenthal et al., 2004; Elderfield et al., 2006; Yu et al., 2007; Yu and Elderfield, 2008; Bian
154 and Martin, 2010; Hasenfratz et al., 2017). Prior to cleaning, foraminifer tests were weighed

and gently crushed between two glass plates under a microscope to allow contaminant phases to be removed during cleaning (Boyle and Keigwin, 1985). If enough material was present, the crushed material was split into two subsamples to allow duplicate measurements. Element/Ca ratios of the cleaned foraminifera material were measured by ICP-MS at ETHZ using a single collector, high-resolution magnetic-sector Thermo Scientific Element XR instrument (see Hasenfratz et al., 2017 for details in cleaning and measuring procedures). The primary standard has been prepared at ETHZ and has a Mg/Ca ratio of 5.59 mmol/mol. The six consistency standards, prepared at the University of Bristol and the University of Cambridge (CL2, CL3, CL4, and CL9; Greaves, 2008), have a composition similar to foraminiferal carbonate (0.51–3.29 mmol/mol of Mg/Ca). They have been measured regularly between August 2014 and August 2016 and are on average within 1.4 % (2 SD; standard deviation) of the gravimetric value for Mg/Ca, with an average long-term reproducibility of ± 2.8 % (2 RSD; relative standard deviation). Duplicate measurements obtained for 36 *Melonis* core top samples, split after crushing and mixing, and before cleaning, show a good reproducibility with 2 SD and 2 RSD of 0.06 mmol/mol and ± 4.2 %, respectively.

Al/Ca, Mn/Ca, and Fe/Mg are used to check for cleaning efficiency (Barker et al., 2003). Contamination is indicated by Mn/Ca higher than 0.25 mmol/mol, which would increase shell Mg/Ca by around ~0.05 mmol/mol and inferred Mg/Ca-temperatures by ~0.5°C, given Mg/Mn ratios in foraminiferal coatings of ~0.2 and a typical Mg/Ca temperature sensitivity of ~0.1 mmol/mol per °C in infaunal benthic foraminifera (Elderfield et al., 2012; Hasenfratz et al., 2017). Moreover, samples with Fe/Ca and Fe/Mg higher than 0.25 mmol/mol and Al/Ca values higher than 0.5 mmol/mol, respectively, were rejected due to potential silicate contamination (Table 1).

2.4 Analytical techniques at the other laboratories

Foraminiferal samples have been cleaned oxidatively (Barker et al., 2003) at GPRL and UoB, and including the reductive step (Boyle and Keigwin, 1985) at INSTAAR. At CU, both

181 approaches were used. Trace metal analysis was performed on a Perkin-Elmer Elan DRC II
182 quadrupole ICP-MS at GLPR (Yu et al., 2005), on a Thermo Finnigan Element 2 ICP-MS at
183 UoB (Rae et al., 2011) and INSTAAR (Marchitto, 2006), and on a Thermo Element XR ICP-
184 MS at CU (Lear et al., 2002, 2010). The long-term precision on Mg/Ca is 1.1 % at INSTAAR,
185 better than 2 % at UoB, and ~2 % at CU and GPRL (2 RSD). Interlaboratory comparisons
186 indicated that the five laboratories ETHZ, GPRL, UoB, INSTAAR and CU agree well with
187 each other. The consistency standards from GPRL and UoB that have been regularly
188 measured at ETHZ are on average within 1.5 % (2 RSD; GPRL) and 1.1 % (2 RSD; UoB) of
189 the gravimetric value for Mg/Ca, indicating that these three laboratories are consistent with
190 each other. GPRL and INSTAAR have both participated in the interlaboratory study from
191 Greaves et al. (2008), with an average offset of 1.4 % (2 RSD). Furthermore, measurement of
192 standards at GPRL and CU indicated that the laboratories in Cambridge and Cardiff agree
193 with each other within analytical error.

194 Potentially contaminated data were rejected using the same thresholds as noted above (Table
195 1). The aspect ratio of the *M. barleeanum* specimens was not quantitatively determined, but
196 the compressed and inflated morphotypes were treated individually at INSTAAR.

197 **2.5 Hydrographic data**

198 Annual averaged bottom water temperature (BWT) (Locarnini et al., 2013) and salinity
199 (Zweng et al., 2013) values for the core top sites were retrieved from World Ocean Atlas
200 2013 (WOA13) version 2 (0.25° grid resolution; 1955−2012). Bottom water $\Delta[CO_3^{2-}]$ was
201 estimated using total CO_2 and total alkalinity (ALK) from the 1° grid resolution dataset
202 provided by Goyet et al. (2000). $[CO_3^{2-}]$ and the saturation state for calcite (Ω) were
203 calculated using CO2calc version 1.3.0 (Robbins et al., 2010), with the dissociation constants
204 K_1 and K_2 as defined by Mehrbach et al. (1973) and refit by Dickson and Millero (1987). The
205 carbonate saturation concentration $[CO_3^{2-}]_{sat}$ was calculated by $[CO_3^{2-}]/\Omega$, and the degree of
206 saturation ($\Delta[CO_3^{2-}]$) was obtained by the difference between $[CO_3^{2-}]$ and $[CO_3^{2-}]_{sat}$. The

207 estimated bottom water temperature, salinity and bottom water $\Delta[CO_3^{2-}]$ at the core top sites
208 used in this study range between −0.9°C and 15.6°C, 34.4 and 36.3 psu, and −2 and 122
209 μmol/kg, respectively (Table 1).

210 ## 3. RESULTS

211 ### 3.1 Morphometric differentiation of *Melonis* species

212 Averages of ARs and number of chambers for each of the core top samples show a bimodal
213 distribution of two distinctively different *Melonis* morphotypes (Fig. 3), with the smaller
214 group having lower AR (~1.1−1.5; spherical type) and a larger group including more
215 compressed tests with higher and more variable ARs (~1.5−2.8). The specimens within the
216 larger group, with an average chamber number of 11.2 ± 1.0, are assigned to *M. barleeanum*.
217 Despite the wide intraspecific range of ARs within *M. barleeanum*, the distribution is nearly
218 Gaussian with a continuous change from relatively inflated to more compressed subtypes. A
219 similar or even larger variability in the AR of *M. barleeanum* was observed by Bergamin et
220 al. (1997) in the Mediterranean Sea (~1.6−2.5), and by Thies (1991) in the North Atlantic
221 (~1.6−3.8), respectively. Secondly, the strongly inflated specimens within the smaller group
222 have an average of 7.2 ± 0.7 chambers in the final whorl. These specimens were collected
223 from water depths of 2000 to 4300 m (Fig. 2). The lesser number of chambers and the
224 occurrence in abyssal depths, together with the low AR, characterize the abyssal plain-
225 inhabiting ecophenotype of *M. pompilioides* (e.g., Holbourn et al., 2013).

226 ### 3.2 Mg/Ca in *Melonis*

227 Following Yu et al. (2007), who found a significant linear correlation between Mg/Ca values
228 resulting from oxidative and reductive cleaning, Mg/Ca values derived from reductively
229 cleaned benthic foraminifera tests are corrected (increased) by a factor of 1.10. Mg/Ca values
230 in *M. barleeanum* range between 0.68 and 2.74 mmol/mol (Fig. 4a) over sites with BWT of
231 −0.9°C to 15.6°C (Table 1). As *M. pompilioides* has only been found in deep water samples at
232 BWT of 0.8–3.5°C (Fig. 2), their Mg/Ca is confined to values of 0.81–1.06 mmol/mol. From

131 analyzed samples, 6 samples were rejected due to potential contamination indicated by elevated Mn/Ca, Fe/Ca, Fe/Mg, and Al/Ca ratios (Table 1). No offset (0.003 ± 0.087 mmol/mol) was found between compressed and inflated *M. barleeanum* co-occurring in three samples (Oslofjord, station 6; GIK8060; GIK16005). A small offset (0.08 ± 0.20 mmol/mol) can be observed between sympatric *M. barleeanum* and *M. pompilioides* measured in five samples (GIK16906, GIK12328, GIK13533, GIK12347, GIK13238), but this offset vanishes if sample GIK13238 (offset of 0.40 mmol/mol) is removed from the statistics (0.01 ± 0.11 mmol/mol) (see also Table 1). The limited number of samples with sympatric *Melonis* specimens of varying morphometry (AR and number of chambers) impedes statistically safe statements on the intra- and interspecific variability of *Melonis*. However, the relatively small Mg/Ca offsets suggest that foraminifera of the genus *Melonis* have a similar temperature response. In general, Mg/Ca ratios and BWT of *Melonis* are relatively well related to each other, defining a linear positive relationship (Fig. 4a).

4. DISCUSSION

4.1 Comparison to published *Melonis* Mg/Ca data

Fig. 4b presents a compilation of *Melonis* Mg/Ca core top data, including data presented in this study and published data from the Norwegian Sea and the Greenland and Iceland shelf (Elderfield et al., 2006; Kristjansdottir et al., 2007; Ezat et al., 2014), the North Atlantic (Lear et al., 2002; Tachikawa and Elderfield, 2004; Marcott et al., 2011), the Bahama Banks, the Gulf of California, and the Pacific Southern Ocean (Lear et al., 2002). For consistency, the Mg/Ca data derived from the full cleaning procedure are corrected by a factor of 1.10 (Yu et al., 2007), and the BWT information is taken from WOA13 for all locations for which Mg/Ca data are presented. As suggested by many studies, the Mg/Ca data from shallow, carbonate-rich sediments of the LBB are not considered in this study as they are very likely contaminated by secondary high-Mg coatings (Reuning et al., 2005; Elderfield et al., 2006; Rosenthal et al., 2006; Marchitto et al., 2007; Regenberg et al., 2007; Curry and Marchitto, 2008; Lear et al., 2008) (see open pink circles in Fig. 4b).

With a few exceptions (Table 1), most of the Mg/Ca data were measured on core top material from the eastern North Atlantic, encompassing the entire latitudinal range from the tropical to the polar realms. Despite the close relationship between Mg/Ca and temperature, the scatter around the linear fit appears to be non-random, with the tropical eastern Atlantic data mostly falling below the regression line (Figs. 4c, 5). As all the tropical Atlantic samples and the majority of the other samples were cleaned oxidatively (Table 1), it is unlikely that their Mg/Ca values were biased during cleaning. Also, like the majority of the samples, they were cleaned at ETH. Furthermore, we can exclude a bias from selected BWT, as *in situ* temperatures measured directly above the core sites of the Gulf of Guinea samples (Lutze et al., 1988) compare very well with the WOA13 temperatures, the latter of which are on average only 0.14°C higher than the former (r^2 = 0.98; p = 4.8 x 10^{-23}; n = 27). In order to further assess the possible cause of variability in the Mg/Ca-BWT relationship, the potential influences on the standardized Mg/Ca residuals are discussed in the following sections.

4.2 Evaluation of the influence of salinity, $\Delta[CO_3^{2-}]$, and morphotype

Bottom water temperature, salinity, and $\Delta[CO_3^{2-}]$ tend to covary over large parts of the deep ocean, generally decreasing with depth. Although it is widely accepted that temperature is the primary control on foraminiferal Mg/Ca, changes in salinity were shown to have a significant effect on planktonic Mg/Ca ratios (e.g., Nürnberg et al., 1996; Ferguson et al., 2008; Hönisch et al., 2013). However, the influence of salinity on benthic foraminifera is debated. While most of the culture (e.g., Toyofuku et al., 2000; Diz et al., 2012) and calibration studies (e.g., Weldeab et al., 2016) have found no salinity effect, an alternative experiment revealed an increase of 3.2–3.6 % in benthic Mg/Ca per salinity unit (Dissard et al., 2010). Bottom water salinity at the sites discussed here (Table 1) ranges from 34.4 to 36.4 psu, but there is no evidence of an influence on the foraminiferal Mg/Ca residuals, when all data are considered (r^2 = 0.02; p = 0.07; n = 154) (Fig. 6a). However, the samples from the eastern tropical Atlantic show a positive correlation between Mg/Ca residual and salinity over a small salinity

range of 0.5 psu (r^2 = 0.40; p = 4.8 x 10^{-5}; n = 35), indicating that salinity might have an influence on the variability observed in the eastern tropical Atlantic data (Fig. 6a).

During the past decade, several studies proposed that bottom water [CO_3^{2-}] affects the incorporation of Mg into epibenthic foraminiferal test carbonate, with lower Mg/Ca ratios in both undersaturated and strongly oversaturated conditions (Rosenthal et al., 2006; Elderfield et al., 2006; Marchitto et al., 2007; Yu and Elderfield, 2008; Lear et al., 2010). The influence of [CO_3^{2-}] on infaunal benthic foraminifera is yet poorly constrained and has been appraised differently. The major uncertainty appears to reside in the estimation of the pore water $\Delta[CO_3^{2-}]$ within the shallow sediment depth the foraminifera are living in. Elderfield et al. (2006; 2010) assumed that the $\Delta[CO_3^{2-}]$ effect weakens with increasing habitat depth in the sediment, based on pore water sampling that indicated rapid equilibration of pore water [CO_3^{2-}] with $CaCO_3$ within the first few centimeters (Martin and Sayles, 1996; 2006). In their view, infaunal foraminifera living a few centimeters below the sediment surface would not be expected to show a $\Delta[CO_3^{2-}]$ effect. This hypothesis has been recently challenged by Weldeab et al. (2016) who have used total alkalinity and pH measurements in pore water from Atlantic sediments (1−10 cm) to show that pore water $\Delta[CO_3^{2-}]$ is lower by about 40–50 µmol/kg compared to the overlying bottom water $\Delta[CO_3^{2-}]$, independently of the saturation state of the overlying bottom waters.

Due to the linear correlation between bottom water and pore water $\Delta[CO_3^{2-}]$ (Weldeab et al., 2016), the bottom water $\Delta[CO_3^{2-}]$ estimates can be used to evaluate the $\Delta[CO_3^{2-}]$ effect on the Mg/Ca ratios of the infaunal foraminifera. Multiple observations indicate that there is likely no systematic effect of $\Delta[CO_3^{2-}]$ on the Mg/Ca ratios of the infaunal *Melonis*. First, Mg/Ca residuals seem to vary independently from their corresponding $\Delta[CO_3^{2-}]$, even at the lowest bottom water $\Delta[CO_3^{2-}]$ values (r^2 = 0.05; p = 0.004; n = 153). Also, although bottom water $\Delta[CO_3^{2-}]$ is lower than 40 µmol/kg for most of the tropical Atlantic sites (and the respective pore water $\Delta[CO_3^{2-}]$ values might even be lower; Weldeab et al., 2016), corresponding to negative Mg/Ca residuals, the overall relationship between their Mg/Ca residuals and

carbonate ion saturation is not consistent (r^2 = 0.03; p = 0.33; n = 35) (Fig. 6b). Secondly, in contrast to studies that have observed distinctly elevated Mg/Ca values in epifaunal *Cibicidoides* from the Nordic Seas, interpreting them as being affected by the anomalously high $\Delta[CO_3^{2-}]$ (Martin et al., 2002a; Elderfield et al., 2006; Yu and Elderfield, 2008), no significant correlation was found in the Nordic Seas samples (r^2 = 0.07; p = 0.06; n = 51). In fact, the Mg/Ca ratios of the 27 Nordic Seas samples that were retrieved below the thermocline (> 500 m; very stable deep water temperatures, but varying $\Delta[CO_3^{2-}]$) have very low Mg/Ca ratios of 0.82 ± 0.11 mmol/mol (Table 1). These observations corroborate the hypothesis laid out by Elderfield et al. (2006) that infaunal foraminifera, such as *Uvigerina* spp. and *Melonis* spp., might be less affected by carbonate ion saturation effects.

As discussed above, the pore water $\Delta[CO_3^{2-}]$ can deviate from that of the bottom water, which, amongst other things, depends on the primary productivity and the remineralization of organic matter within the upper sediment (e.g., Emerson et al., 1982; Martin and Sayles, 1996; Weldeab et al., 2016). In general, *M. barleeanum* has been associated with a high-productivity regime in the surface ocean (Mackensen et al., 1985; Lutze et al., 1986; Mackensen et al., 1993; Schmiedl et al., 1997; Rudolph, 2006). Their maximum abundances are centered at flux rates of 3 to 10 g C m^{-2} yr^{-1} particulate organic carbon (Altenbach et al., 1999). Information on core top organic carbon content was only available for 40 % of the core tops, including the majority of the tropical Atlantic sites (Müller, 1975; Diester-Haass and Peter, 1979; Mackensen, 1985; Lutze et al., 1986; Tiedemann, 1986; Westerhausen et al., 1993) and some of the Norwegian Sea (Mackensen et al., 1985; Hoff et al., 2016), the northern North Atlantic (Austin and Evans, 2000; Thomson et al., 2000), and the Pacific Southern Ocean sites (Wagner et al., 2013). In general, seafloor organic matter flux and total organic carbon (TOC) is higher at the northwestern African margin and the eastern equatorial Atlantic than at the other sites (Fig. 6c). Given the availability of oxygen in pore waters, remineralization of organic matter might depress pore water $\Delta[CO_3^{2-}]$ compared to the already relatively low bottom water values due to increased bacterial respiration. Interestingly, in this

study, a trend between the sedimentary TOC and the Mg/Ca residuals has been found, irrespective of the *Melonis* species (all data: $r^2 = 0.31$; $p = 2.2 \times 10^{-6}$; $n = 62$; tropical Atlantic: $r^2 = 0.17$; $p = 0.02$; $n = 33$). Although the evidence is weak, and, for instance, the lability of the organic matter is not taken into account, the negative relationship between tropical Atlantic Mg/Ca residuals and TOC might suggest that benthic foraminifera from sediments experiencing high organic matter fluxes and increased production of CO_2 by remineralizing bacteria have altered Mg/Ca ratios due to a fractionation effect during calcification in undersaturated pore waters (Martin et al., 2002b; Yu and Elderfield, 2008) or due to preferential (post-mortem) dissolution of Mg-rich parts of the carbonate (McCorkle et al., 1995; Martin et al., 2005). As the investigated *Melonis* specimens did not show any apparent dissolution features, the former scenario is more likely. Another aspect that might alter the relationship between organic matter flux and Mg/Ca residual is the change in the depth habitat of *Melonis* as *M. barleeanum* was shown to migrate deeper in the sediment during times of increased food availability. However, because pore water $\Delta[CO_3^{2-}]$ does not show a clear decline below ~1–2 cm and remains relatively stable (Weldeab et al., 2016), we conclude that the potential vertical migration of *Melonis* spp. has a negligible influence on the $\Delta[CO_3^{2-}]$ effect.

Finally, we assessed if varying morphotypes of *M. barleeanum* can explain some of the variation in the Mg/Ca residuals. Comprehensive, quantitative morphometric information is only available for the samples investigated at ETHZ/MPIC. In general, there is a relatively large variation in the AR within regions, but there is a tendency of more compressed types corresponding to more negative Mg/Ca residuals ($r^2 = 0.27$; $p = 1.9 \times 10^{-7}$; $n = 89$), specifically for the eastern tropical Atlantic samples ($r^2 = 0.42$; $p = 1.3 \times 10^{-4}$; $n = 29$) (Fig. 6d). As initial measurements on a small set of sympatric *M. barleeanum* morphotypes indicated that there is probably no intraspecific offset, we suspect that the reason for this correlation is spurious. It is possible that the relationship between morphotype and Mg/Ca residual may be partly controlled by the causal connection between aspect ratio of *M.*

367 *barleeanum* and organic matter flux (with the latter potentially affecting pore water $\Delta[CO_3^{2-}]$
368 as discussed above). In previous studies, it was found that more compressed morphotypes of
369 *M. barleeanum* are more abundant in upwelling regions such as the northwestern African
370 margin, while the more inflated types are found predominantly in low-productivity areas or
371 during periods of food scarcity, probably due to a link between habitus and food supply
372 (Thies, 1991; Altenbach et al., 1993; Bhaumik et al., 2014). Although there is indeed a weak
373 positive trend between TOC and aspect ratio of *M. barleeanum* in our dataset ($r^2 = 0.22$; $p = 6.7 \times 10^{-4}$; $n = 49$; plot not shown), it is difficult to assess the causality between the two
374
375 parameters given the limited number of samples.

376 In summary, the evaluation of our data indicates that bottom water $\Delta[CO_3^{2-}]$ and varying
377 morphotype cannot explain the variability of the Mg/Ca-BWT data. However, the relatively
378 high TOC contents in sediments below high-productive regions could be an indicator for
379 lowered pore water $\Delta[CO_3^{2-}]$ that might provide an explanation for the relatively low Mg/Ca
380 residuals for most of the eastern tropical Atlantic samples. In contrast to the entire dataset,
381 there seems to be a salinity effect in the tropical Atlantic data, but the relatively narrow
382 salinity range makes it difficult to conclusively assess its influence. Last, although we cannot
383 exclude that the specimens from the tropical Atlantic and the other regions (Table 1) represent
384 different cryptic species of *M. barleeanum* and *M. pompilioides*, which respond to BWT in a
385 differential way, the similar reaction in Mg/Ca ratios of the two *Melonis* species renders this
386 scenario unlikely.

387 **4.3 Calibration**

388 In order to construct a reliable Mg/Ca-temperature calibration, it is important that all data
389 included are robust (Fig. 4b). To ensure that the different laboratories where the data have
390 been produced are consistent with each other, it was decided to only use data that have been
391 newly acquired for this project (80 % of all available data on *Melonis* spp.), and all other data
392 are used for comparison. Multiple regression analysis of these 125 data points detected four

393 data points whose standardized residuals are higher than ± 3σ (with very high Cook's
394 distances of > 0.14; Cook and Weisberg, 1982), and one data point with a residual ± 2.6σ
395 (Cook's *D* of 0.08). These outliers cannot be explained by environmental parameters, such as
396 salinity or $\Delta[CO_3^{2-}]$. The standardized residual threshold to reject data designated for
397 temperature calibrations varies in the literature from ± 1σ (e.g., Kim et al., 2008) to ± 3σ (e.g.,
398 Conte et al., 2006), or when Cook's *D* greatly exceeds 4/n, with n being the number of
399 samples (0.032 for this dataset) (e.g., Mackay et al., 2003). The threshold mostly used in
400 foraminiferal Mg/Ca paleothermometry is ± 2σ, which should comprise ~95% of the data
401 (e.g., Rathmann et al., 2004; Haarmann et al., 2011; Quillmann et al., 2012). Given that the
402 remaining 120 data all have residuals within the ± 1.7σ range and within 0.03 of Cook's
403 distance, the five data points with residuals larger than ± 2σ (Cook's *D* larger than 0.08) were
404 removed from the calibration data set in order to prevent the outliers exerting undue leverage
405 on the final statistical estimates (see Table 1).

406 In contrast to previous calibrations that have found (weak) evidence for an exponential
407 response of *Melonis* Mg/Ca to temperature (Lear et al., 2002; Kristjansdottir et al., 2007), the
408 data are best explained by a linear relationship, with a sensitivity of 0.11 mmol/mol Mg/Ca
409 per °C (Fig. 4d):

$$Mg/Ca = 0.113 \pm 0.005\,T + 0.792 \pm 0.036 \;\; (r^2 = 0.81;\ \mathrm{n} = 120;\ 1\sigma\ SD) \qquad (1)$$

410 The calibration uncertainty increases with increasing Mg/Ca, resulting into a 1σ temperature
411 error of ± 0.3 °C and ± 1.0 °C for temperatures around -1 °C and 16 °C, respectively.

412 In a foraminiferal Mg/Ca interlaboratory study, Rosenthal et al. (2004) showed that a large
413 part of the variability was due to the application of different cleaning methods, concluding
414 that a consistent protocol would improve the comparability of Mg/Ca results. The calibration
415 dataset consists of 13 samples that have gone through the full cleaning procedure, including
416 reductive cleaning that has been shown to decrease foraminiferal Mg/Ca values (e.g.,
417 Elderfield et al., 2006; Yu et al., 2007). In this study, we correct for this bias in benthic

418 Mg/Ca values using the linear fit between samples that were oxidatively and reductively
419 cleaned, respectively, as given by Yu et al. (2007). Their comparison is based on *Cibicidoides*
420 and *Uvigerina* species, which might have a different susceptibility to the corrosive cleaning
421 solution than *Melonis* species. The amount of Mg-enriched carbonate preferentially dissolved
422 from the foraminifer tests depends on many factors (e.g., porosity, homogeneity of the Mg
423 distribution, amount of coating, degree of crushing before cleaning), and the correction might
424 introduce additional uncertainty (Quillmann et al., 2012). However, we consider that the
425 added uncertainty is minimal. First, although the coefficient is based on three different
426 benthic genera, their effect on the reductive cleaning is very similar (r^2 = 0.93) (Yu et al.,
427 2007). Second, the effect of the reductive cleaning in the interlaboratory study from Rosenthal
428 et al. (2004) is relatively consistent for the foraminifera used (r^2 = 0.97), indicating that a
429 coefficient determined in one lab can be applied for data produced in other laboratories. Last,
430 discarding the reductively cleaned samples would not change the sensitivity of the calibration
431 presented in this study, resulting into a small temperature difference (~0.2−0.4 °C) that is
432 within the uncertainty of the calibration. This suggests that the coefficient used to correct
433 reductively cleaned data can also reliably be applied for *Melonis* spp.. Similarly, excluding
434 the samples from the tropical Atlantic that might be partly biased by lowered pore water
435 $\Delta[CO_3^{2-}]$ (or might have a salinity effect) would not affect the slope of the linear fit, but
436 would change the intercept leading to temperature differences of ~0.4−1.2 °C. Because the
437 evidence of a possible bias is small, we recommend using the calibration equation that
438 includes all the data. In Fig. 4d, the different calibration equations are compared to each other.

439 The previously published data (excluding the LBB samples) compare relatively well to the
440 new data, except for five data points from the Nordic Seas (Kristjansdottir et al., 2007;
441 Elderfield et al., 2006) that have relatively high Mg/Ca residuals (Figs. 4b, 5a). Concerning
442 the three data points from Kristjansdottir et al. (2007), we suspect that the reason for the high
443 residuals are temperature uncertainties, as discussed in the initial calibration study. In detail,
444 the BWT obtained from CTD casts at the core top locations during the B997 cruise in July

1997 (Kristjansdottir et al., 2007) and temperatures sourced from WOA13 were found to differ by more than 2 °C for 4 of the 15 sites (2.87 ± 0.68 °C) on the Iceland shelf (with the three mentioned sites, 314, 315 and 337, among these four sites). Bottom water temperatures on the Iceland shelf, where warmer Atlantic waters converge with southward flowing polar waters, are known to vary significantly on a seasonal to annual time-scale (e.g., Malmberg and Jonsson, 1997).

The sensitivity obtained for *Melonis* species is very similar to sensitivities found in other benthic taxa (Elderfield et al., 2006; Marchitto et al., 2007; Lear et al., 2010; Quillmann et al., 2012), in between the one for the infaunal *Uvigerina* species often used for BWT reconstructions (Elderfield et al., 2006; Bryan and Marchitto, 2008; Elderfield et al., 2010; 2012, Roberts et al., 2016) and species with high Mg content and higher sensitivities, such as *Globobulimina* spp. (Weldeab et al. 2016) and *Hyalinea balthica* (Rosenthal et al., 2011).

5. CONCLUSIONS

Infaunal benthic foraminifera of the genus *Melonis* populate all ocean basins from low to high latitudes, and from the shelf to abyssal depth, and are hence well-suited proxy carriers in paleoceanography. However, existing temperature reconstructions using Mg/Ca ratios of *Melonis* depend upon calibrations that suffer from significant uncertainties. In this study, we have compiled a novel data set, based on new data mostly from the North Atlantic, together with published data. This allows us to establish a Mg/Ca-temperature calibration of high quality extending from −1°C to 16°C described by Mg/Ca (mmol/mol) = 0.113 ± 0.005T + 0.792 ± 0.036. Although the limited number of samples with sympatric *Melonis* specimens of varying morphometry makes it difficult to conclusively assess the intra- and interspecific variability of *Melonis*, the relatively small Mg/Ca offsets between sympatric morphotypes suggests that foraminifera of the genus *Melonis* have a similar temperature response. The large deviation between data from the LBB (Lear et al., 2002) and all other data in the compiled data set provides further evidence that *Melonis* tests from the LBB are contaminated

and do not yield Mg/Ca values representative of the original ontogenetic shell. Mg/Ca ratios of the analyzed tests show no strong dependence to bottom water $\Delta[CO_3^{2-}]$. However, *Melonis* from the tropical eastern Atlantic core top sites that experience high organic carbon flux show lower Mg/Ca than tests from other sites, which might be an indicator of lower pore water $\Delta[CO_3^{2-}]$ affecting the fractionation of Mg during calcification.

Acknowledgments

We acknowledge the financial support provided by ETH Research Grant ETH-04 11-1 (A.P.H.), and the Swiss National Science Foundation grants PZ00P2_141424 (A.M.-G.) and PP00P2_144811 (S.L.J.). We are very greatful to James Rae, Harry Elderfield, and Mervyn Greaves for making unpublished data available, Karen Louise Knudsen for providing Oslofjord samples, Stéphane Westermann and Corey Archer for support with the solution-based ICP-MS analyses, Antje Sorowka for taking the SEM images at MPIC, and Julia Gottschalk who made the multi-lab collaboration possible.

References

Altenbach A. V., Heeger T., Linke P., Spindler M. and Thies A. (1993) *Miliolinella subrotunda* (Montagu), a miliolid foraminifer building large detritic tubes for a temporary epibenthic lifestyle. *Mar. Micropaleontol.* **20**, 293–301.

Altenbach A. V., Pflaumann U., Schiebel R., Thies A., Timm M. and Trauth M. (1999) Scaling percentages of benthic foraminifera with flux rates of organic carbon. *J. Foraminif. Res.* **29**, 173–185.

Altenbach A. V., Lutze G. F., Schiebel R. and Schönfeld J. (2003) Impact of interrelated and interdependent ecological controls on benthic foraminifera: an example from the Golf of Guinea. *Palaeogeog. Palaeoclimatol. Palaeoecol.* **144**, 3–19.

Austin W. E. N. and Evans J. R. (2000) NE Atlantic benthic foraminifera: modern distribution patterns and palaeoecological significance. *J. Geol. Soc. London* **157**, 679–691.

496 Barker S., Greaves M., and Elderfield H. (2003) A study of cleaning procedures used for
497 foraminiferal Mg/Ca paleothermometry. *Geochem. Geophys. Geosyst.* **4**,
498 doi:10.1029/2003GC000559.

499 Bauch D. and Bauch H. A. (2001) Last glacial benthic foraminiferal $\delta^{18}O$ anomalies in the
500 polar North Atlantic: a modern analogue evaluation. *J Geophys. Res.* **106**, 9135–9143.

501 Belanger P. E. and Streeter S. S. (1980) Distribution and ecology of benthic foraminifera in
502 the Norwegian-Greenland Sea. *Mar. Micropaleontol.* **5**, 401–428.

503 Bergamin L., Carboni M. G. and Di Bella L. (1997) *Melonis pompilioides* (Fichtel and Moll)
504 and *Melonis barleeanus* (Williamson) from Pliocene, Pleistocene and Holocene sediments of
505 Central Italy. *Geologica Romana* **33**, 29–45.

506 Berggren W. A., Benson R. H., Haq B. U., Riedel W. R., Sanfilippo A., Schrader H.-J. and
507 Tjalsma R. C. (1976) The El Cuervo section (Andalusia, Spain): micropaleontologic anatomy
508 of an early Late Miocene lower bathyal deposit, *Mar. Micropaleontol.* **1***,* 195–247.

509 Berggren W. A. and Kaminski M. A. (1990) Abyssal agglutinates: Back to basics, In
510 *Paleoecology, Biostratigraphy, Paleoceanography and Taxonomy of Aggluginated*
511 *Foraminifera* (eds. C. Hemleben et al.), Kluwer, Dordrecht, Netherlands, pp. 53–75.

512 Bhaumik A. K., Gupta A. K., Clemens S. C. and Mazumder R. (2014) Functional morphology
513 of *Melonis barleeanum* and *Hoeglundina elegans*: a proxy for water-mass characteristics.
514 *Current Science* **106**, 1123–1140.

515 Bian N. and Martin P. A. (2010) Investigating the fidelity of Mg/Ca and other elemental data
516 from reductively cleaned planktonic foraminifera. *Paleoceanography* **25**, PA2215.

517 Boltovskoy E. (1958) Problems in taxonomy and nomenclature exemplified by *Nonion affinis*
518 (Reuss). *Micropaleont*. **4**, 193–200.

519 Boyle E. A. and Keigwin L. D. (1985) Comparison of Atlantic and Pacific paleochemical
520 records for the last 215,000 years: Changes in deep ocean circulation and chemical
521 inventories. *Earth Planet. Sci. Lett.* **76**, 135–150.

522 Bryan S. P. and Marchitto T. M. (2008) Mg/Ca-temperature proxy in benthic foraminifera:
523 New calibrations from the Florida Straits and a hypothesis regarding Mg/Li.
524 *Paleoceanography* ***23***, PA2220.

525 Conte M. H., Sicre M. A., Rühlemann C., Weber J. C., Schulte S., Schulz-Bull D. and Blanz
526 T. (2006) Global temperature calibration of the alkenone unsaturation index ($U^{K'}_{37}$) in surface
527 waters and comparison with surface sediments. *Geochem. Geophys. Geosyst*. **7**, Q02005.

528 Cook D. R. and Weisberg S. (1982) Residuals and influence in regression. Chapman & Hall,
529 New York, USA, 230 pp.

530 Corliss B. H. (1979) Taxonomy of recent deep-sea benthonic foraminifera from the southeast
531 Indian Ocean, *Micropaleont.* **25**, 1–19.

532 Curry W. B. and Marchitto T. M. (2008) A secondary ionization mass spectrometry
533 calibration of *Cibicidoides pachyderma* Mg/Ca with temperature. *Geochem. Geophys.*
534 *Geosyst.* **9**, Q04009.

535 Dickson A. G. and Millero F. J. (1987) A comparison of the equilibrium constants for the
536 dissociation of carbonic acid in seawater media. *Deep-Sea Res. A Oceanogr. Res. Pap.* **34**,
537 1733–1743.

538 Diester-Haass L. and Müller P. J. (1979) Processes influencing sand fraction composition and
539 organic matter content in surface sediments off W Africa (12−19°N). *'Meteor'*
540 *Forschungsergebnisse, Reihe C: Geologie und Geophysik* **31**, 21–48.

541 Dissard D., Nehrke G, Reichart G. J. and Bijma J. (2010) The impact of salinity on the Mg/Ca
542 and Sr/Ca ratio in the benthic foraminifera *Ammonia tepida*: Results from culture

543 experiments. *Geochim. Cosmochim. Acta* **74**, 928–940.

544 Diz P., Barras C., Geslin E., Reichart G.-J., Metzger E., Jorissen F. J., Bijma J. (2012)
545 Incorporation of Mg and Sr and oxygen and carbon stable isotope fractionation in cultured
546 *Ammonia tepida*. *Mar. Micropaleontol.* **92–93**, 16–28.

547 Dokken T. M. and Jansen E. (1999) Rapid changes in the mechanism of ocean convection
548 during the last glacial period, *Nature* **401**, 458–461.

549 Elderfield H., Yu J., Anand P., Kiefer T. and Nyland B. (2006) Calibrations for benthic
550 foraminiferal Mg/Ca paleothermometry and the carbonate ion hypothesis. *Earth Planet. Sci.*
551 *Lett.* **250**, 633–649.

552 Elderfield H., Greaves M., Barker S., Hall I. R., Tripati A., Ferretti P., Crowhurst S., Booth L.
553 and Daunt C. (2010) A record of bottom water temperature and seawater $\delta^{18}O$ fort he
554 Southern Ocean over the past 440 kyr based on Mg/Ca of benthic foraminiferal *Uvigerina*
555 spp.. *Quat. Sci. Rev.* **29**, 160–169.

556 Elderfield H., Ferretti P., Greaves M., Crowhurst S., McCave I. N., Hodell D. and Piotrowski
557 A. M. (2012) Evolution of ocean temperature and ice volume through the Mid-Pleistocene
558 climate transition. *Science* **337**, 704–709.

559 Emerson S., Grundmanis V. and Graham D. (1982) Carbonate chemistry in marine pore
560 waters: MANOP sites C and S. *Earth Planet. Sci. Lett.* **61**, 220–232.

561 Ezat M. M., Rasmussen T. L. and Groeneveld J. (2014) Persistent intermediate water
562 warming during cold stadials in the southeastern Nordic seas during the past 65 k.y.. *Geology*
563 **42**, 663–666.

564 Ferguson J. E., Henderson G. M., Kucera M. and Rickaby R. E. M. (2008) Systematic change
565 of foraminiferal Mg/Ca ratios across a strong salinity gradient. *Earth Planet. Sci. Lett.* **265**,
566 153–166.

567 Fontanier C., Jorissen F. J., Licari L., Alexandre A., Anschutz P. and Carbonel P. (2002) Live
568 benthic foraminiferal faunas from the Bay of Biscay: faunal density, composition, and
569 microhabitats. *Deep-Sea Research,* **49**, 751–785.

570 Fontanier C., Mackensen A., Jorissen F. J., Anschutz P., Licari L. and Griveaud C. (2006)
571 Stable oxygen and carbon isotopes of live benthic foraminifera from the Bay of Biscay:
572 Microhabitat impact and seasonal variability. *Mar. Micropaleontol.* **58**, 159–183.

573 Goyet C., Healy R. J. and Ryan J. P. (2000) Global distribution of total inorganic carbon and
574 total alkalinity below the deepest winter mixed layer depths. ORNL/CDIAC-127, NDP-076,
575 Carbon Dioxide Information Analysis Center, Oak Ridge National Laboratory, U. S.
576 Department of Energy, Oak Ridge, Tennessee.

577 Greaves M., Caillon N., Rebaubier H., Bartoli G., Bohaty S., Cacho I., Clarke L., Cooper M.,
578 Daunt C., Delaney M., deMenocal P., Dutton A., Eggins S., Elderfield H., Garbe-Schönberg
579 D., Goddard E., Green D., Groeneveld J., Hastings D., Hathorne E., Kimoto K., Klinkhammer
580 G., Labeyrie L., Lea D. W., Marchitto T., Martinez-Boti M. A., Mortyn P. G., Ni Y.,
581 Nürnberg D., Paradis G., Pena L., Quinn T., Rosenthal Y., Russell A., Sagawa T., Sosdian S.,
582 Stott L., Tachikawa K., Tappa E., Thunell R., Wilson P. A. (2008) Interlaboratory comparison
583 study of calibration standards for foraminiferal Mg/Ca thermometry. *Geochem. Geophys.*
584 *Geosyst.* **9**, Q08010.

585 Greaves M. J. (2008) Trace elements in marine biogenic carbonates: Analysis and application
586 to past ocean chemistry. PhD Thesis, Univ. of Southampton, Southampton, UK, 194 pp.

587 Haake F. W. (1980) Benthische Foraminiferen in Oberflächen-Sedimenten und Kernen des
588 Ostatlantiks vor Senegal/Gambia (Westafrika). *'Meteor' Forschungsergebnisse, Reihe C:*
589 *Geologie und Geophysik*, **32**, 1–29.

590 Haarmann T., Hathorne E. C., Mohtadi M., Groeneveld J., Kölling M. and Bickert T. (2011)
591 Mg/Ca ratios of single planktonic foraminifer shells and the potential to reconstruct the

592 thermal seasonality of the water column. *Paleoceanography* **26**, PA3218.

593 Hasenfratz A. P., Martinez-Garcia A., Jaccard S. L., Vance D., Wälle M., Greaves M. and
594 Haug G. H. (2017) Determination of the Mg/Mn ratio in foraminiferal coatings: an approach
595 to correct Mg/Ca temperatures for Mn-rich contaminant phases. *Earth Planet. Sci. Lett.* **457**,
596 335–347.

597 Hoff U., Rasmussen T. L., Stein R., Ezat M. M. and Fahl, K. (2016) Sea ice and millennial-
598 scale climate variability in the Nordic seas 90 kyr ago to present. *Nature Commun.* **7**, 1–29.

599 Hönisch B., Allen K. A., Lea D. W., Spero H. J., Eggins S. M., Arbuszewski J., deMenocal
600 P., Rosenthal Y., Russell A. D. and Elderfield H. (2013) The influence of salinity on Mg/Ca
601 in planktic foraminifers—Evidence from cultures, core-top sediments and complementary
602 $\delta^{18}O$. *Geochim. Cosmochim. Acta* **121***,* 196–213.

603 Holbourn, A., A. S. Henderson, and N. MacLeod (2013) *Atlas of Benthic Foraminifera*,
604 Wiley-Blackwell, UK, 642 pp.

605 Jones R. W. (1994) *The Challenger Foraminifera*. The Natural History Museum, London,
606 Oxford University Press, UK, 149 pp.

607 Jorissen F. J., Wittling I., Peypouquet J. P., Rabouille C. and Relexans J. C. (1998) Live
608 benthic foraminiferal faunas off Cape Blanc, NW-Africa: Community structure and
609 microhabitats. *Deep-Sea Res. I* **45**, 2157–2188.

610 Kim J.-H., van der Meer J., Schouten S., Helmke P., Willmott V., Sangiorgi F., Koc N.,
611 Hopmans E. C. and Sinninghe Damsté J. S. (2010) New indices and calibrations derived from
612 the distribution of crenarchaeal isoprenoid tetraether lipids: Implications for past sea surface
613 temperature recontructions. *Geochim. Cosmochim. Acta* **74**, 4639–4654.

614 Kristjansdottir G. B., Lea D. W., Jennings A. E., Pak D. K. and Belanger C. (2007) New
615 spatial Mg/Ca temperature calibrations for three Arctic, benthic foraminifera and

reconstruction of north Iceland shelf temperature for the past 4000 years. *Geochem. Geophys. Geosyst.* **8**, Q03P21.

Lear C., Rosenthal Y. and Slowey N. (2002) Benthic foraminiferal Mg/Ca paleothermometry: a revised core-top calibration. *Geochim. Cosmochim. Acta* **66**, 3375–3387.

Lear C. H., Bailey T. R., Pearson P. N., Coxall H. K. and Rosenthal Y. (2008) Cooling and ice growth across the Eocene-Oligocene transition. *Geology* **36**, 251–254.

Lear C. H., Mawbey E. M., and Rosenthal Y. (2010) Cenozoic benthic foraminiferal Mg/Ca and Li/Ca records: Toward unlocking temperatures and saturation states. *Paleoceanography* **25**, PA4215.

Linke P. and Lutze G. F. (1993) Microhabitat preferences of benthic foraminifera – a static concept or a dynamic adaptation to optimize food acquisition? In *Foraminiferal Microhabitats* (ed. M. R. Langer), *Mar. Micropaleontol.* **20**, 215–234.

Lo Guidice Capelli E., Regenberg M., Holbourn A., Kuhnt W., Garbe-Schönberg D. and Andersen N. (2015) Refining *C wuellerstorfi* and *H. elegans* Mg/Ca temperature calibrations. *Mar. Micropaleontol.* **21**, 70–84.

Locarnini R. A., Mishonov A. V., Antonov J. I., Boyer T. P., Garcia H. E., Baranova O. K., Zweng M. M., Paver C. R., Reagan J. R., Johnson D. R., Hamilton M. and Seidov D. (2013) *World Ocean Atlas 2013, Volume 1: Temperature* (ed. S. Levitus, technical ed. A. Mishonov), NOAA Atlas NESDIS **73**, 40 pp.

Lutze G. F., Sarnthein M., Koopmann B. and Pflaumann U. (1979) Meteor Core 12309: Late Pleistocene reference section for interpretation of the Neogene of Site 397. *Initial Rep. Deep Sea Drill. Proj.* **47**, 727–739.

Lutze G. F. and Coulbourn W. T. (1984) Recent benthic foraminifera from the continental margin of Northwest Africa: Community structure and distribution. *Mar. Micropaleontol.* **8**,

361–401.

Lutze G. F., Pflaumann U. and Weinholz P. (1986) Jungquartäre Fluktuationen der benthischen Foraminiferenfaunen in Tiefsee-Sedimenten vor NW-Afrika. Eine Reaktion auf Produktivitätsveränderungen im Oberflächenwasser. *'Meteor' Forschungsergebnisse, Reihe C: Geologie und Geophysik* **40**, 63–180.

Lutze G. F., Agwu C. O. C., Altenbach A., Henken Mellies U., Kothe C., Mühlhahn N., Pflaumann U., Samtleben C., Sarnthein M., Segl M., Soltwedel T., Stute U., Tiedemann R. and Weinholz P. (1988) Bericht über die "Meteor"- Fahrt 6-5, Dakkar-Libreville 15.1-16.2.1988, Berichte Geologisches Paläontologisches Institut Universität Kiel **22**, 66 pp.

Mackay A. W., Battarbee R. W., Flower R. J., Granin N. G., Jewson D. H., Ryves D. B., and Sturm M. (2003) Assessing the potential for developing internal diatom-based transfer function for Lake Baikal **48**, 1183–1192.

Mackensen A. (1985) Verbreitung und Umwelt benthischer Foraminiferen in der Norwegischen See. PhD Thesis, Geologisch-Paläontologisches Institut der Christian-Albrechts-Universität Kiel, 126 pp.

Mackensen A., Sejrup H. P. and Jansen E. (1985) The distribution of living and dead benthic foraminifera on the continental slope and rise off southwest Norway. *Mar. Micropaleontol.* **9**, 275–306.

Mackensen A., Fütterer D. K., Grobe H. and Schmiedl G. (1993). Benthic foraminiferal assemblages from the eastern South Atlantic Polar Front region between 35° and 57°S: Distribution, ecology and fossilization potential. *Mar. Micropaleontol.* **22**, 33–69.

Mackensen A., Schmiedl G., Harloff J. and Giese M. (1995) Deep-Sea Foraminifera in the South Atlantic Ocean: Ecology and Assemblage Generation. *Micropaleontol.* **41**, 342–358.

Malmberg S.-A. and Jonsson S. (1997) Timing of deep convection in the Greenland and

664 Iceland Seas. *ICES J. Mar. Sci.* **54**, 300–309.

665 Marchitto T. M. (2006) Precise multi-elemental ratios in small foraminiferal samples
666 determined by sector field ICP-MS, *Geochem. Geophys. Geosyst.* **7**, Q05P13.

667 Marchitto T. M., Bryan S. P., Curry W. B. and Mc-Corkle D. C. (2007) Mg/Ca temperature
668 calibration for the benthic foraminifer *Cibicioides pachyderma*. *Paleoceanography* **22**,
669 PA1203.

670 Marcott S. A., Clark P. U., Padman L., Klinkhammer G. P., Springer S. R., Liu Z., Otto-
671 Bliesner B. L., Carlson A. E., Ungerer A., Padman J., He F., Cheng J. and Schmittner A.
672 (2011) Ice-shelf collapse from subsurface warming as a trigger for Heinrich events. *Proc.*
673 *Natl. Acad. Sci. U.S.A.* **108**, 13415–13419.

674 Martin P. A. and Lea D. W. (2002) A simple evaluation of cleaning procedures on fossil
675 benthic foraminiferal Mg/Ca. *Geochem. Geophys. Geosyst.* **3**, 8401.

676 Martin P. A., Lea D. W., Rosenthal Y., Shackleton N. J., Sarnthein M. and Pappenfuss T.
677 (2002a), Quaternary deep sea temperature histories derived from benthic foraminiferal
678 Mg/Ca. *Earth Planet. Sci. Lett.* **198**, 193–209.

679 Martin P. A., Lea D. W. and McCorkle D. C. (2002b) Examining the evidence for the
680 influence of carbonate saturation state on benthic foraminiferal Mg/Ca. *Eos Trans. AGU* **83**,
681 Fall Meet. Suppl., Abstract PP52B-12.

682 Martin P., Archer, D. and Lea D. W. (2005) Role of deep sea temperature in the carbon cycle
683 during the last glacial. *Paleoceanography* **20**, doi: 10.1029/2003PA000914.

684 Martin W. R., and Sayles F. L. (1996) $CaCO_3$ dissolution in sediments of the Ceara Rise,
685 western equatorial Atlantic. *Geochim. Cosmochim. Acta* **60**, 243–263.

686 Martin W. R., and Sayles F. L. (2006) Organic matter oxidation in deep-sea sediments:

687 distribution in the sediment column and implications for calcite dissolution. *Deep-Sea Res. II*
688 **52**, 771–792.

689 McCorkle D., Martin P. A., Lea D. W. and Klinkhammer G. P. (1995) Evidence of a
690 dissolution effect on benthic foraminiferal shell chemistry: $\delta^{13}C$, Cd/Ca, Ba/Ca, and Sr/Ca
691 results from the Ontong Java Plateau. *Paleoceanography* **10**, 699–714.

692 Mead G. A. (1985), Recent benthic foraminifera in the Polar Front Region of the Southwest
693 Atlantic. *Microplaeontol.* **31**, 221–248.

694 Mehrbach C., Culberso C. H., Hawley J. E. and Pytkowic R. M. (1973) Measurement of
695 apparent dissociation constants of carbonic acid in seawater at atmospheric pressure. *Limnol.*
696 *Oceanogr.* **18**, 897–907.

697 Meland M. Y., Dokken T. M., Jansen E. and Hevroy K. (2008) Water mass properties and
698 exchange between the Nordic seas and the northern North Atlantic during the period 23-6 ka:
699 Benthic oxygen isotopic evidence. *Paleoceanography.* **23**, PA1210.

700 Milker Y. and Schmiedl G. (2012) A taxonomic guide to modern benthic shelf foraminifera
701 of the western Mediterranean Sea. *Palaeontologica Electronica* **15**, 1–134.

702 Müller P. J. (1975), Diagenese stickstoffhaltiger organischer Substanzen in oxischen und
703 anoxischen marinen Sedimenten. *'Meteor' Forschungsergebnisse, Reihe C: Geologie und*
704 *Geophysik* **22**, 1–60.

705 Nürnberg D., Bijma J. and Hemleben C. (1996) Assessing the reliability of magnesium in
706 foraminiferal calcite as a proxy for water mass temperature. *Geochim. Cosmochim. Acta* **60**,
707 803–814.

708 Quillmann U., Marchitto T. M., Jennings A. E., Andrews J. T. and Friestad B. F. (2012)
709 Cooling and freshening at 8.2 ka on the NW Iceland Shelf recorded in paired $\delta^{18}O$ and Mg/Ca
710 measurements of the benthic foraminifer *Cibicides lobatulus*. *Quat Res.* **78**, 528–539.

711 Rae J. W. B., Foster G. L., Schmidt D. N. and Elliott T. (2011) Boron isotopes and B/Ca in
712 benthic foraminifera: proxies for the deep ocean carbonate system. *Earth Planet. Sci. Lett.*
713 **302**, 403–413.

714 Rathmann S., Hess S., Kuhnert H. and Mulitza S. (2004) Mg/Ca ratios of the benthic
715 foraminifera *Oridorsalis umbonatus* obtained by laser ablation from core top sediments:
716 Relationship to bottom water temperature. *Geochem. Geophys. Geosyst.* **5**, Q12013.

717 Regenberg M., Nürnberg D., Schönfeld J. and Reichart G.-J. (2007) Early diagenetic
718 overprint in Caribbean sediment cores and its effect on the geochemical composition of
719 planktonic foraminifera. *Biogeosciences* **4**, 957–973.

720 Reuning L., Reijmer J. J. G., Betzler C., Swart P. and Bauch T. (2005) The use of
721 paleoceanographic proxies in carbonate periplatform settings—opportunities and pitfalls.
722 *Sedimentary Geology* **175**, 131–152.

723 Risdal D. (1964), Foraminiferfaunaens relation til dybdeforholdene i Oslofjorden, med en
724 diskusjon av de senkvartære foraminifersoner. *Norges Geologiske Undersøkelse* **226**, 1–142.

725 Robbins L. L., Hansen M. E., Kleypas, J. A. and Meylan S.C. (2010) CO2calc − A user-
726 friendly seawater carbon calculator for Windows, Max OS X, and iOS (iPhone): U.S.
727 Geological Survey Open-File Report 2010 − 1280, 17 pp.

728 Roberts J., Gottschalk J., Skinner L. C., Peck V. L., Kender S., Elderfield H., Waelbroeck C.,
729 Vazquez Riveiros N. and Hodell D. A. (2016) Evolution of South Atlantic density and
730 chemical stratification across the last deglaciation. *Proc. Natl. Acad. Sci. U.S.A.* **113**, 514–
731 519.

732 Rosenthal Y., Boyle E. A. and Slowey, N. (1997) Temperature control on the incorporation of
733 magnesium, strontium, fluorine, and cadmium into benthic foraminiferal shells from Little
734 Bahama Bank: Prospects for thermocline paleoceanography. *Geochim. Cosmochim. Acta* **61**,

735 3633–3643.

736 Rosenthal Y., Perron-Cashman S., Lear C. H., Bard E., Barker S., Billups K., Bryan M.,
737 Delaney M. L., deMenocal P. B., Dwyer G. S., Elderfield H., German C. R., Greaves M., Lea
738 D. W., Marchitto Jr. T. M., Pak D. K., Paradis G. L., Russell A. D., Schneider R. R.,
739 Scheiderich K., Stott L., Tachikawa K., Tappa E., Thunell R., Wara M., Weldeab S., Wilson
740 P. A. (2004) Interlaboratory comparison study of Mg/Ca and Sr/Ca measurements in
741 planktonic foraminifera for paleoceanographic research. *Geochem. Geophys. Geosyst.* **5**,
742 Q04D09.

743 Rosenthal Y., Lear C. H., Oppo D. W. and Linsley B. K. (2006) Temperature and carbonate
744 ion effects on Mg/Ca and Sr/Ca ratios in benthic foraminifera: Aragonitic species
745 *Hoeglundina elegans*. *Paleoceanography* **21**, PA1007.

746 Rosenthal Y., Morley A., Barras C., Katz M. E., Jorissen F., Reichart G.-J., Oppo D. W. and
747 Linsley K. L. (2011) Temperature calibration of Mg/Ca ratios in the intermediate water
748 benthic foraminifer *Hyalinea balthica*. *Geochem. Geophys. Geosyst.* **12**, Q04003.

749 Rudolph M. (2006) Benthische Foraminiferenvergesellschaftungen als Anzeiger für
750 spätquartäre Positionsänderungen der Fronten des Antarktischen Zirkumpolarstroms im
751 Südatlantik, *Berichte zur Polar- und Meeresforschung* **522**, PhD Thesis, 149 pp.

752 Schiebel R. (1992) Rezente benthische Foraminiferen in Sedimenten des Schelfes und oberen
753 Kontinentalhanges im Golf von Guinea (Westafrika). Berichte Geologisch-Paläontologisches
754 Institut der Universität Kiel **51**, PhD Thesis, 179 pp.

755 Schmiedl G., Mackensen A. and Müller P. J. (1997) Recent benthic foraminifera from the
756 eastern South Atlantic Ocean: dependence on food supply and water masses. *Mar.*
757 *Micropaleontol.* **32**, 249–288.

758 Schmiedl G. and Mackensen A. (2006) Multispecies stable isotopes of benthic foraminifers

759 reveal past changes of organic matter decomposition and deepwater oxygenation in the
760 Arabian Sea. *Paleoceanography* **21**, PA4213.

761 Schönfeld J. (2001) Benthic foraminifera and pore water oxygen profiles: a re-assessment of
762 species boundary conditions at the western Iberian margin. *J. Foraminif. Res.* **31**, 86–107.

763 Schönfeld J., and Altenbach A. V. (2005) Late Glacial to Recent distribution pattern of deep-
764 water *Uvigerina* species in the north-eastern Atlantic. *Mar. Micropaleontol.* **57**, 1–24.

765 Schumacher S. (2001) Mikrohabitatansprüche benthischer Foraminiferen in Sedimenten des
766 Südatlantiks, *Berichte zur Polar- und Meeresforschung* **403**, PhD Thesis, 151 pp.

767 Seiler W. C. (1975) Tiefenverteilung benthischer Foraminiferen am portugiesischen
768 Kontinentalhang. *'Meteor' Forschungsergebnisse, Reihe C: Geologie und Geophysik* **23**, PhD
769 Thesis, 47–94.

770 Tachikawa K. and Elderfield H. (2004) Chemistry of benthic foraminiferal shells for
771 recording ocean environments: Cd/Ca, $\delta^{13}C$ and Mg/Ca, In *Environmental Change in the*
772 *Ocean and on Land* (eds. M. Shiyomi et al.), Terrapub, Japan, pp. 249–263.

773 Thies A. (1991), Die Benthos-Foraminiferen im Europäischen Nordmeer, *Berichte aus dem*
774 *Sonderforschungsbereich 313*, Christian-Albrechts-Universität Kiel **31**, PhD Thesis, 97 pp.

775 Thomson J., Brown L., Nixon S., Cook G. T. and MacKenzie A. B. (2000) Bioturbation and
776 Holocene sediment accumulation fluxes in the north-east Atlantic Ocean (Benthic Boundary
777 Layer experiment sites). *Mar. Geol.* **169**, 21–39.

778 Thornalley D. J. R., Elderfield H. and McCave, I. N. (2010) Intermediate and deep water
779 paleoceanography of the northern North Atlantic over the past 21,000 years.
780 *Paleoceanography* **25**, PA1211.

781 Tiedemann R. (1986) Verteilung von organischem Kohlenstoff in Oberflächensedimenten

und örtliche Primärproduktion im äquatorialen Ostatlantik, 0−20°N, 15−25°W. Diploma Thesis, Christian-Albrechts-Universität Kiel, 75 pp.

Timm S. (1992) Rezente Tiefseeforaminiferen aus Oberflächensedimenten des Golfes von Guinea (Westafrika) – Taxonomie, Verbreitung, Ökologie und Korngrössenfraktionen. *Berichte Geologisch-Paläontologisches Institut der Universität Kiel* **59**, PhD Thesis, 192 pp.

Toyofuku T., Kitazato H., Kawahata H., Tsuchija M. and Nohara, M. (2000) Evaluation of Mg/Ca thermometry in foraminifera: Comparison of experimental results and measurements in nature. *Paleoceanography* **15**, 456–464.

van Morkhoven F. P. C. M., Berggren W. A. and Edwards A. S. (1986) Cenozoic Cosmopolitan Deep-Water Benthic Foraminifera. *Bull. Cent. Rech. Explor. Prod. Elf. Aquitaine* **11**, 421 pp.

Waelbroeck C., Labeyrie L., Michel E., Duplessy J. C., McManus J. F., Lambeck K., Balbon E. and Labracherie M. (2002) Sea-level and deep water temperature changes derived from benthic foraminifera isotopic records. *Quat. Sci. Rev.* **21**, 295–305.

Wagner M., Hendy I. L., McKay J. L. and Pedersen, T. F. (2013) Influence of biological productivity on silver and redox-sensitive trace metal accumulation in Southern Ocean surface sediments, Pacific Sector. *Earth Planet. Sci. Lett.* **380**, 31–40.

Weldeab S., Arce A. and Kasten S. (2016) Mg/Ca-$\Delta CO_3^{2-}{}_{\text{pore water}}$-temperature calibration for *Globobulimina* spp.: A sensitive paleothermometer for deep-sea temperature reconstruction. *Earth Planet. Sci. Lett.* **438**, 95–102.

Westerhausen L., Poynter J., Eglington G., Erlenkeuser K. and Sarnthein M. (1993) Marine and terrigenous origin of organic matter in modern sediments of the equatorial east Atlantic: The $\delta^{13}C$ and molecular record. *Deep-Sea Res. I* **40**, 1087–1121.

Wright R., College B. and Wisconsin B. (1978) Neogene paleobathymetry of the

Mediterranean based on benthic foraminifers from DSDP Leg 42A. *Initial Rep. Deep Sea Drill. Proj.* **42**, 837–846.

Yu J. M., Day J., Greaves M. and Elderfield H. (2005) Determination of multiple element/calcium ratios in foraminiferal calcite by quadropole ICP-MS. *Geochem. Geophys. Geosyst.* **6**, Q08P01.

Yu J., Elderfield H., Greaves M. and Day, J. (2007) Preferential dissolution of benthic foraminiferal calcite during laboratory reductive cleaning. *Geochem. Geophys. Geosyst.* **8**, Q06016.

Yu J., and Elderfield H. (2008) Mg/Ca in benthic foraminifera *Cibicidoides wuellerstorfi* and *Cibicidoides mundulus*: Temperature versus carbonate ion saturation. *Earth Planet. Sci. Lett.* **276**, 129–139.

Zweng M. M, Reagan J. R., Antonov J. I., Locarnini R. A., Mishonov A. V., Boyer T. P., Garcia H. E., Baranova O. K., Johnson D. R., Seidov D. and Biddle M. M. (2013) *World Ocean Atlas 2013, Volume 2: Salinity* (Ed. S. Levitus, Technical Ed. A. Mishonov), NOAA Atlas NESDIS **74**, 39 pp.

821 **1 Table, 6 Figures.**

822 **Table 1.** Location, bottom water properties, relative abundance, and Mg/Ca of core top
823 *Melonis* presented in this study, ordered by oceanic region and decreasing latitude.

Core[a]	Lat (°N)	Lon (°E)	Depth (m)	BWT[b] (°C)	BWS[b] (psu)	ΔCO_3^{2-}[c] (µmol/kg)	Species[d] *Melonis* ...	Total[e]	Abun.[f] (%)	Mg/Ca[g] (mmol/mol)	Institute/ Cleaning[h]
Nordic Seas											
GIK23004	67.733	5.920	1244	-0.86	34.91	51.9	*barl.*	881	0.2	0.84	ETHZ - O
GIK23001	67.700	3.832	1257	-0.89	34.91	51.5	*barl.*	119	0.8	0.77	ETHZ - O
GIK23040	67.003	7.780	967	-0.63	34.91	57.7	*barl.*	159	2.5	0.79	ETHZ - O
GIK23008	66.932	7.917	840	-0.60	34.92	56.3	*barl.*	914	3.0	0.69	ETHZ - O
GS19MCA	63.760	5.190	922	-0.72	34.91	74.6	*barl.*			0.90	CU - O
GIK16119	63.431	3.129	1403	-0.83	34.91	49.0	*barl.*	211	12.0	0.79	ETHZ - O
GIK16120	63.275	3.210	1205	-0.81	34.91	53.7	*barl.*	578	15.0	0.78	ETHZ - O
GIK16142	63.152	2.362	1100	-0.83	34.91	55.1	*barl.*	310	42.0	0.76	ETHZ - O
GIK16121	63.124	3.049	1003	-0.85	34.92	56.8	*barl.*	304	47.0	0.71	ETHZ - O
GIK16107	63.098	0.343	1497	-0.84	34.91	42.1	*barl.*	120	2.0	1.05	ETHZ - O
GIK16143	63.093	2.496	1002	-0.79	34.91	57.0	*barl.*	275	46.0	0.79	ETHZ - O
GIK16144	63.049	2.592	900	-0.76	34.91	53.4	*barl.*	210	77.0	0.74	ETHZ - O
GIK16122	63.043	3.203	900	-0.80	34.92	53.4	*barl.*	307	61.0	0.73	ETHZ - O
GIK16106	63.036	0.476	1304	-0.80	34.91	45.2	*barl.*	198	16.0	0.77	ETHZ - O
KN177-2 MC11	63.032	0.807	1285	-0.80	34.91	45.6	*barl.*			0.91	CU - R
GS04-138-21	62.860	-6.130	652	-0.24	34.91	82.0	*barl.*			1.00	INSTAAR - R
GS15MCA[3]	62.860	-6.11	592	-0.14	34.90	90.8	*barl.*			0.98	CU - O
GS16MCA	62.840	-6.17	550	0.04	34.90	92.2	*barl.*			1.05	CU - O
KN177-2 MC14	62.819	1.300	965	-0.74	34.91	55.8	*barl.*			0.89	CU - R
KN177-2 MC6	62.604	1.744	695	-0.47	34.91	57.0	*barl.*			0.83	CU - R
GIK16145	62.590	3.141	803	-0.65	34.92	53.8	*barl.*	211	56.0	0.73	ETHZ - O
GIK16105	62.566	1.020	1100	-0.80	34.91	55.1	*barl.*	365	8.0	0.68	ETHZ - O
GIK16123	62.529	3.427	801	-0.70	34.92	53.8	*barl.*	394	78.0	0.76	ETHZ - O
GIK16146	62.516	3.300	693	-0.74	34.91	56.8	*barl.*	99	35.0	0.74	ETHZ - O
GIK16124	62.468	3.537	605	-0.35	34.91	60.4	*barl.*	294	26.0	0.96	ETHZ - O
GIK16147	62.462	3.431	607	-0.32	34.91	60.3	*barl.*	156	54.0	0.89	ETHZ - O
GIK16149	62.410	3.536	401	5.46	35.10	75.1	*barl.*	205	1.0	1.52	ETHZ - O
MC56E	62.402	3.137	380	2.77	34.98	90.3	*barl.*			1.35	CU - O
GIK16150	62.390	3.591	293	7.15	35.21	84.4	*barl.*	229	1.0	1.84	ETHZ - O
GIK16151	62.380	4.002	205	7.85	35.25	87.3	*barl.*	110	1.0	1.77	ETHZ - O
GIK16104	62.369	1.434	702	-0.49	34.91	73.8	*barl.*	394	56.0	0.77	ETHZ - O
GIK16152	62.183	4.396	144	8.09	35.21	88.7	*barl.*	294	6.0	2.05	ETHZ - O
KN177-2 MC4	62.120	2.721	418	5.15	35.08	73.6	*barl.*			1.21	CU - R
GIK16103	62.074	2.432	410	5.70	35.09	75.0	*barl.*	248	17.0	1.18	ETHZ - O
Oslofjord (Risdal, 1964)											
Station 35	59.650	10.617	100	7.20	34.90	74.0	*barl.*			2.03	INSTAAR - R
Station 21	59.333	10.617	220	6.66	35.14		*barl.*			2.00	INSTAAR - R
Station 20	59.317	10.550	155	6.88	35.07	78.8	*barl.*			1.79	INSTAAR - R
Station 11[2]	59.283	10.650	50	8.03	34.36	64.1	*barl.*			2.16	INSTAAR - R
Station 11[2]	59.283	10.650	50	8.03	34.36	64.1	*barl.* fat			3.43	INSTAAR - R
Station 6	59.267	10.658	105	7.17	34.92	74.2	*barl.*			1.63	INSTAAR - R
Station 6	59.267	10.658	105	7.17	34.92	74.2	*barl.* fat			1.53	INSTAAR - R
Subtropical to northern North Atlantic											
RapiD-10-1P	62.976	-15.590	1237	4.47	35.00	66.3	*barl.*			1.51	GLPR - O
RapiD-4-2C	61.739	-15.402	2284	3.08	34.97	46.9	*barl.*			1.39	GLPR - O
RapiD-17-5P	61.482	-19.536	2303	2.95	34.99	36.8	*barl.*			1.30	CU - O
GIK16202	60.475	-8.744	330	8.77	35.32	98.7	*barl.*	96	10.4	1.35	ETHZ - O
GIK16205	60.332	-12.628	305	8.58	35.27	100.7	*barl.*	31	29.0	2.02	ETHZ - O
GIK16204	60.139	-13.358	609	8.13	35.25	96.3	*barl.*	33	6.1	1.82	ETHZ - O
GIK16201	59.601	-7.714	904	7.26	35.27	84.6	*barl.*	155	0.6	1.69	ETHZ - O
RapiD-32-22B	58.249	-47.012	3096	2.08	34.91	34.3	*barl.*			1.18	CU - O
RapiD-35-25B	57.508	-48.723	3486	1.80	34.90	28.0	*barl.*			1.10	CU - O
GIK16213	57.158	-13.019	1207	5.66	35.10	72.6	*barl.*	173	2.9	1.38	ETHZ - O
GIK16214	57.105	-13.200	638	8.86	35.32	89.5	*barl.*	196	1.0	1.98	ETHZ - O
GIK16220	52.699	-14.868	709	9.54	35.37	68.4	*barl.*	142	1.4	1.79	ETHZ - O
GIK16901	49.285	-11.416	410	10.95	35.53	95.2	*barl.* mix	268	2.2	2.25	ETHZ - O
GIK16901	49.285	-11.416	410	10.95	35.53	95.2	*barl.* fat			2.09	ETHZ - O
GIK16906	49.010	-13.567	3889	2.51	34.91	12.3	*barl.*	171	2.9	1.18	ETHZ - O
GIK16906	49.010	-13.567	3889	2.51	34.91	12.3	*pomp.*	171	0.0	1.05	ETHZ - O
GIK10792	40.500	-9.655	1268	10.38	36.11	86.8	*barl.*	65	2.0	1.88	ETHZ - O
GIK10809	40.325	-9.572	182	12.82	35.78	111.0	*barl.*	363	1.1	2.39	ETHZ - O
GIK10810	40.325	-9.452	146	13.16	35.83	114.6	*barl.* mix	386	0.8	2.34	ETHZ - O
GIK10802[4]	40.303	-9.785	816	11.53	36.09	82.5	*barl.*	385	1.6	3.63	ETHZ - O

GIK10808	40.303	-9.618	211	12.60	35.75	108.0	*barl.*	251	4.8	2.27	ETHZ - O
GIK10805	40.292	-9.667	377	11.59	35.61	93.0	*barl.*	115	2.6	1.99	ETHZ - O
GIK10801	40.280	-9.845	1010	11.22	36.15	83.3	*barl.*	103	3.9	1.81	ETHZ - O
GIK10807	40.280	-9.632	238	12.42	35.72	105.3	*barl.* mix	35	4.0	2.18	ETHZ - O
GIK10806	40.270	-9.643	287	12.05	35.66	100.8	*barl.*	217	6.5	1.96	ETHZ - O
GIK10770	37.708	-9.375	618	12.12	36.01	83.9	*barl.*	406	18.5	2.13	ETHZ - O
GIK8060	37.692	-9.500	996	11.59	36.28	73.6	*barl.*	104	6.7	2.19	ETHZ - O
GIK8060	37.692	-9.500	996	11.59	36.28	73.6	*barl.* fat			2.26	ETHZ - O
GIK8011	37.689	-9.255	500	11.78	35.77	87.5	*barl.*	204	9.3	1.90	ETHZ - O
GIK10769	37.683	-9.475	611	12.10	36.00	83.9	*barl.*	70	2.8	2.65	ETHZ - O
GIK10767	37.675	-9.717	1709	6.41	35.45	49.9	*barl.*	165	1.8	1.61	ETHZ - O
GIK10777	37.638	-8.973	148	14.34	36.02	121.5	*barl.* mix	610	1.0	2.59	ETHZ - O
GIK10774	37.612	-9.283	600	12.07	35.97	84.0	*barl.* fat	214	7.0	2.26	ETHZ - O
GIK15809	35.962	-7.314	945	10.40	35.87	69.0	*barl.* fat	131	1.5	2.12	ETHZ - O
GIK15659[2]	34.893	-6.758	285	13.43	35.86	104.2	*barl.* mix	37	2.7	2.56	ETHZ - O
GIK15658	34.887	-6.703	205	14.46	36.11	114.0	*barl.*	289	0.7	2.33	ETHZ - O
GIK15653	34.870	-6.602	140	15.43	36.25	115.6	*barl.*	146	0.7	2.33	ETHZ - O
GIK15652	34.868	-6.582	130	15.58	36.26	115.5	*barl.*	101	2.0	2.47	ETHZ - O
GIK15678	33.472	-12.750	4305	2.46	34.90	-1.9	*pomp.*	156	*1.1	0.98	ETHZ - O
GIK15644[4]	32.398	-9.808	485	11.76	35.63	81.5	*barl.*	86	1.2	3.64	ETHZ - O
GIK15644	32.398	-9.808	485	11.76	35.63	81.5	*barl.* fat			2.78	ETHZ - O
GIK15645[4]	32.383	-9.783	440	12.13	35.68	86.0	*barl.*	99	*3.3	3.66	ETHZ - O
GIK15645[4]	32.383	-9.783	440	12.13	35.68	86.0	*barl.* fat			3.26	ETHZ - O
GIK16005	29.247	-11.507	811	9.18	35.42	47.2	*barl.*			1.87	ETHZ - O
GIK16005	29.247	-11.507	811	9.18	35.42	47.2	*barl.* fat			1.89	ETHZ - O
GIK15634	28.255	-13.395	1215	6.70	35.27	39.0	*barl.* fat	353	0.8	1.84	ETHZ - O
GIK15635	27.203	-14.660	2605	3.10	34.97	25.4	*pomp.*	306	*0.7	1.07	ETHZ - O
GIK12306	26.327	-14.928	741	6.59	35.27	42.4	*barl.*	65	3.1	1.83	ETHZ - O
Tropical North Atlantic											
GIK12328	21.145	-18.573	2822	2.78	34.95	17.3	*barl.*	94	5.3	0.85	ETHZ - O
GIK12328	21.145	-18.573	2822	2.78	34.95	17.3	*pomp.*	94	2.1	0.91	ETHZ - O
GIK13533	20.993	-18.032	2112	3.46	34.99	26.0	*barl.*	115	14.8	1.02	ETHZ - O
GIK13533	20.993	-18.032	2112	3.46	34.99	26.0	*pomp.*	115	0.9	0.99	ETHZ - O
GIK12347	15.825	-17.845	2710	2.88	34.94	24.7	*barl.*	133	3.8	0.80	ETHZ - O
GIK12347	15.825	-17.845	2710	2.88	34.94	24.7	*pomp.*	133	2.3	0.92	ETHZ - O
GIK12346	15.570	-17.545	1517	4.38	34.97	29.0	*barl.*	171	*0.5	0.86	ETHZ - O
GIK13237	14.118	-17.640	996	5.80	34.87	32.5	*barl.*	334	8.4	1.13	ETHZ - O
GIK13238	14.097	-17.875	1983	3.52	34.97	29.6	*barl.*	286	10.1	0.94	ETHZ - O
GIK13238	14.097	-17.875	1983	3.52	34.97	29.6	*pomp.*	286	0.0	0.54	ETHZ - O
GIK16420	9.928	-17.533	806	5.84	34.70	10.8	*barl.*	100	3.0	1.05	ETHZ - O
GIK16753	9.583	-16.543	457	8.95	34.97	16.6	*barl.*	189	4.8	1.61	ETHZ - O
GIK16754	9.503	-16.623	646	6.79	34.73	10.0	*barl.*	149	1.3	1.17	ETHZ - O
GIK16755	9.253	-16.858	1002	5.12	34.75	31.2	*barl.*	195	1.0	1.05	ETHZ - O
GIK16762	8.395	-14.413	302	11.49	35.17	34.0	*barl.*	105	1.0	2.74	ETHZ - O
GIK16850[4]	6.102	3.670	247	12.39	35.23	45.6	*barl.*	133	3.8	3.60	ETHZ - O
GIK16852	6.072	3.643	770	5.23	34.55	20.0	*barl.*	199	1.5	0.97	ETHZ - O
GIK16853	6.065	3.642	1018	4.56	34.67	62.3	*barl.*	153	4.6	0.94	ETHZ - O
GIK16844[1]	5.720	1.160	1230	4.43	34.86	69.3	*barl.*	252	0.8	0.90	ETHZ - O
GIK16845[1]	5.557	1.150	2007	3.50	34.95	74.8	*barl.*	192	3.6	0.68	ETHZ - O
GIK16846	5.365	1.287	2739	2.90	34.92	56.6	*barl.*	239	1.3	0.75	ETHZ - O
GIK16813	5.008	-4.547	297	10.83	35.04	36.5	*barl.* fat	132	2.3	2.22	ETHZ - O
GIK16806	4.950	-4.553	1204	4.45	34.81	62.5	*barl.*	183	4.4	0.96	ETHZ - O
GIK16801	4.520	-6.473	310	10.56	35.01	34.1	*barl.*	164	0.6	2.01	ETHZ - O
GIK16786	4.512	-9.147	451	7.98	34.75	30.5	*barl.*	110	8.2	1.87	ETHZ - O
GIK16820	4.503	-2.303	445	8.06	34.76	17.0	*barl.*	190	5.8	1.45	ETHZ - O
GIK16787	4.482	-9.195	674	5.90	34.60	24.9	*barl.*	152	3.3	1.05	ETHZ - O
GIK16819	4.453	-2.335	631	6.12	34.60	13.5	*barl.*	150	6.0	1.09	ETHZ - O
GIK16799	4.447	-6.433	1505	4.11	34.94	43.1	*barl.*	154	4.5	0.91	ETHZ - O
GIK16818	4.388	-2.367	749	5.34	34.56	12.9	*barl.*	177	1.1	0.94	ETHZ - O
GIK16831	4.350	-1.152	632	6.02	34.58	13.3	*barl.*	132	1.5	1.36	ETHZ - O
GIK16798	4.345	-6.402	2221	3.20	34.95	42.4	*barl.*	138	0.7	0.74	ETHZ - O
GIK16817	4.322	-2.383	1001	4.56	34.65	25.0	*barl.*	158	1.3	0.91	ETHZ - O
GIK16796	4.101	-6.268	3296	2.52	34.90	23.1	*pomp.*	256	0.0	0.81	ETHZ - O
GIK16861	3.622	6.500	403	8.74	34.78	26.3	*barl.*	123	3.3	1.29	ETHZ - O
GIK16862	3.547	6.487	698	5.54	34.55	27.5	*barl.*	167	3.6	0.96	ETHZ - O
GIK16863	3.397	6.415	993	4.57	34.65	60.4	*barl.*	165	1.2	0.88	ETHZ - O
Eastern South Atlantic											
GeoB12808-4	-26.370	11.892	3796	1.79	34.82	21.2	*barl.*			1.20	UoB - O
Sulawesi margins											
BJ8-03MC24	-5.065	117.448	832	5.18	34.55	2.5	*barl.*			1.41	CU - R
BJ8-03MC29	-3.894	119.370	987	4.72	34.56	15.1	*barl.*			1.56	CU - R
BJ8-03MC22	-3.887	119.495	1189	4.13	34.57	10.9	*barl.*			1.90	CU - R
Pacific Southern Ocean											
PS75/073-2	-57.204	-151.611	3234	0.77	34.71	2.5	*pomp.*			0.82	ETHZ - O

824

[a] Rejected samples have a superscript next to their core name: 1 = high Fe/Ca and/or Fe/Mg; 2 = high Mn/Ca; 3 = high Al/Ca; 4 = outlier (>2σ).

[b] Temperature (Locarnini et al., 2013) and salinity (Zweng et al., 2013) data are from WOA13.

[c] Calculation of ΔCO_3^{2-} is explained in detail in the text.

[d] The abbreviations '*barl.*' and '*pomp.*' stands for *barleeanum* and *pompilioides*. The different morphotypes of *M. barleeanum* are distinguished: '*barl.*' = compressed to transitional; '*barl.* fat' = spherical; '*barl.* mix' = compressed to spherical.

[e] Total sum of counted benthic specimens in the >250 µm fraction (Seiler, 1975; Haake, 1980; Lutze and Coulbourn, 1984; Mackensen et al., 1985; Thies, 1991; Timm, 1992; Schiebel, 1992; Altenbach et al., 1999; Altenbach et al. 2003; Schönfeld and Altenbach, 2005).

[f] Abundance of living *M. barleeanum* (all morphotypes) and *M. pompilioides* relative to all benthic foraminifera species in the >250 µm fraction. The asteriks mark samples where the relative abundance was determined on the dead assemblage. See reference in [e].

[g] Mg/Ca values of samples cleaned reductively are corrected (increased) by factor 1.10 (Yu et al., 2007).

[h] Samples were processed at {ETHZ = ETH Zurich; GLPR = University of Cambridge; INSTAAR = University of Colorado; CU = Cardiff University; UoB = University of Bristol} using {O = oxidative cleaning; R = oxidative and reductive cleaning}.

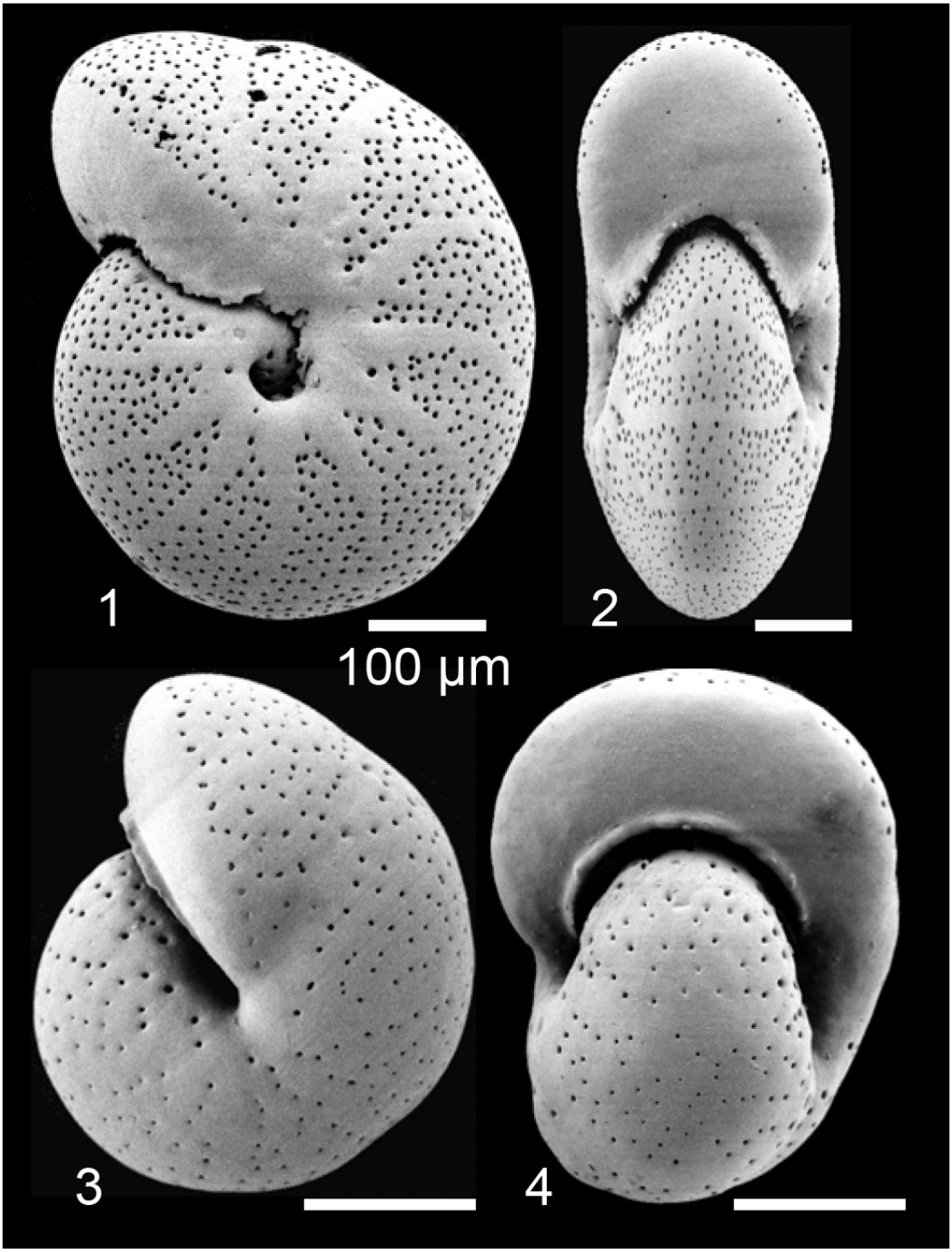

844

845 **Figure 1.** *Melonis barleeanum* (1, 2) and *Melonis pompilioides* (3, 4) in lateral (1, 3) and
846 frontal (2, 4) view. Both specimens are from sediments of ODP Site 1094 (77.55 mcd). All
847 scale bars are 100 µm.

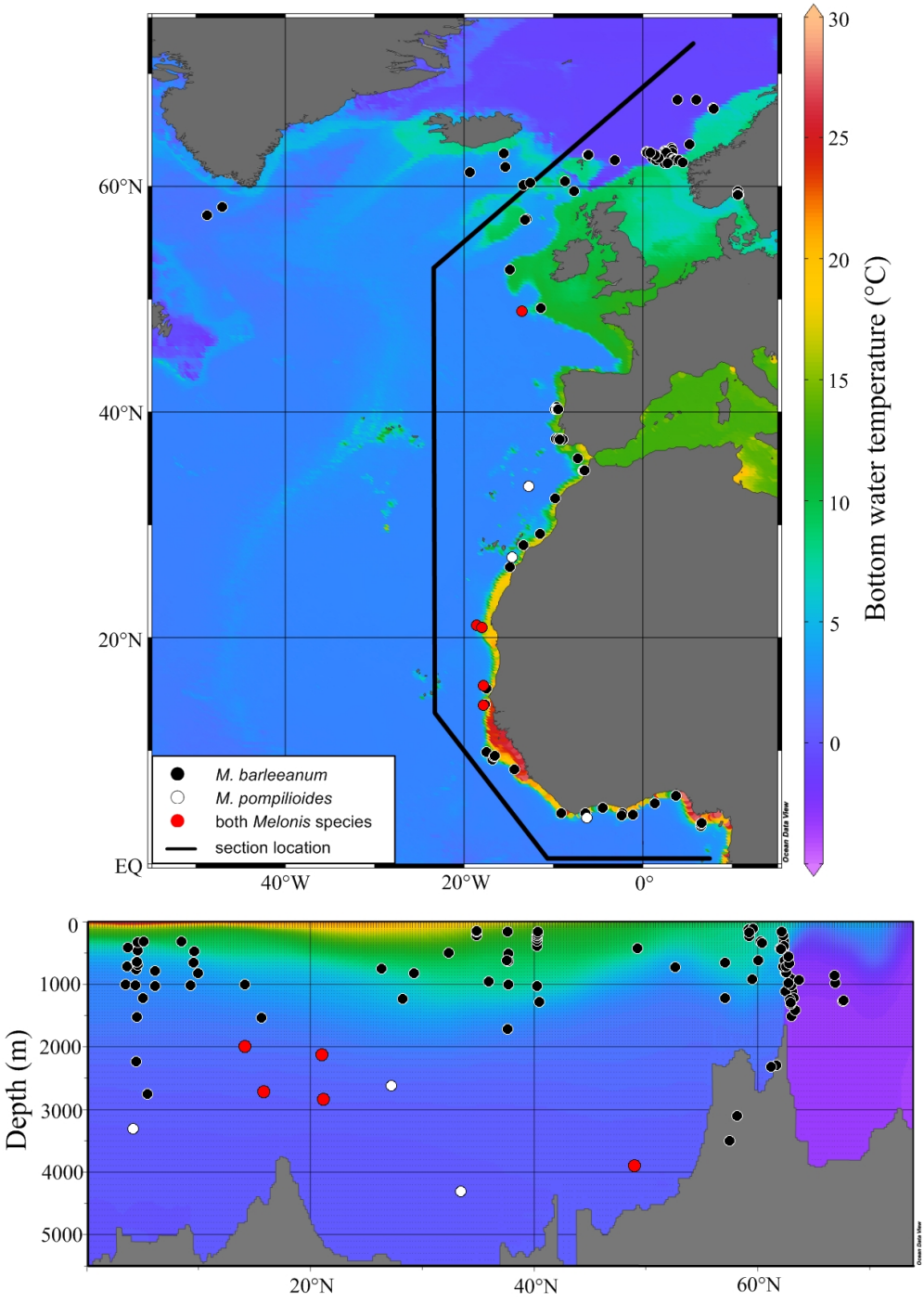

848

849 **Figure 2.** Locations of North Atlantic core top samples investigated in this study shown on a
850 surface map and a latitudinal transect depicting bottom water temperature. Sample locations
851 cover a large range of oceanographic conditions in the North Atlantic spanning -0.9°C
852 (Norwegian Sea) to 15.6°C (shallow site off Morocco). In addition to the sites shown on the
853 map, three core tops from the Sulawesi margin, one core top from the South Atlantic and one
854 core top from the Pacific Southern Ocean were analyzed (see Table 1).

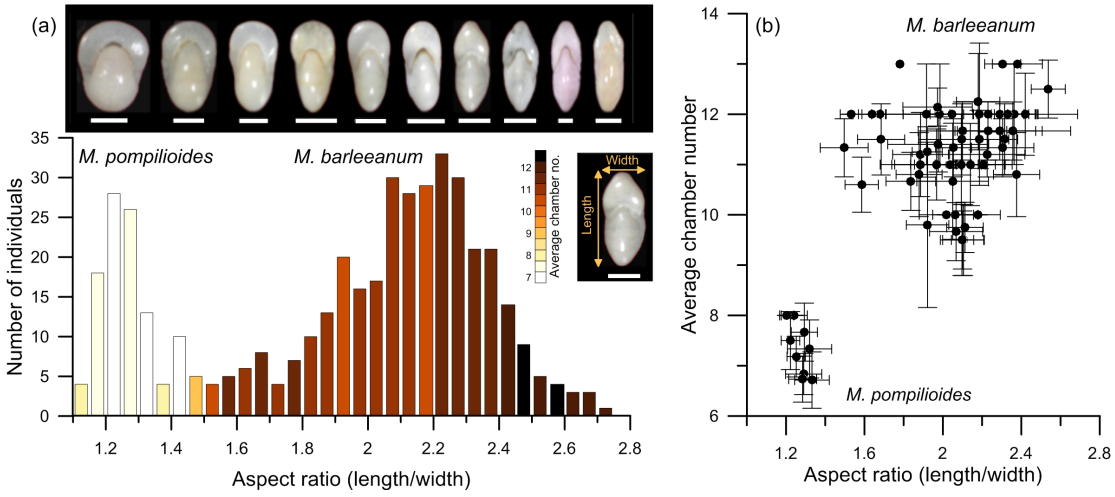

855

856 **Figure 3.** (a) Histogram of the aspect ratio (length/width) of the *Melonis* specimens processed
857 at ETHZ/MPIC (black symbols in Fig. 4a) showing two peaks centered around 2.2 (*M.*
858 *barleeanum*) and 1.25 (*M. pompilioides*), respectively. The average chamber number,
859 spanning between 7 (pale yellow) and 13 (dark red), varies with the aspect ratio. At the top,
860 characteristic *Melonis* morphotypes are depicted in frontal view with their aspect ratio
861 roughly corresponding to the x-axis below (from left to right: GIK13533, GIK15809,
862 GIK10774, GIK10774, GIK10774, GIK16119, GIK10774, GIK16861, GIK16853,
863 GIK13533). Note that the second test from the right is Rose Bengal stained. (b) Relationship
864 between aspect ratio and chamber number for the core tops investigated. All scale bars are
865 200 µm.

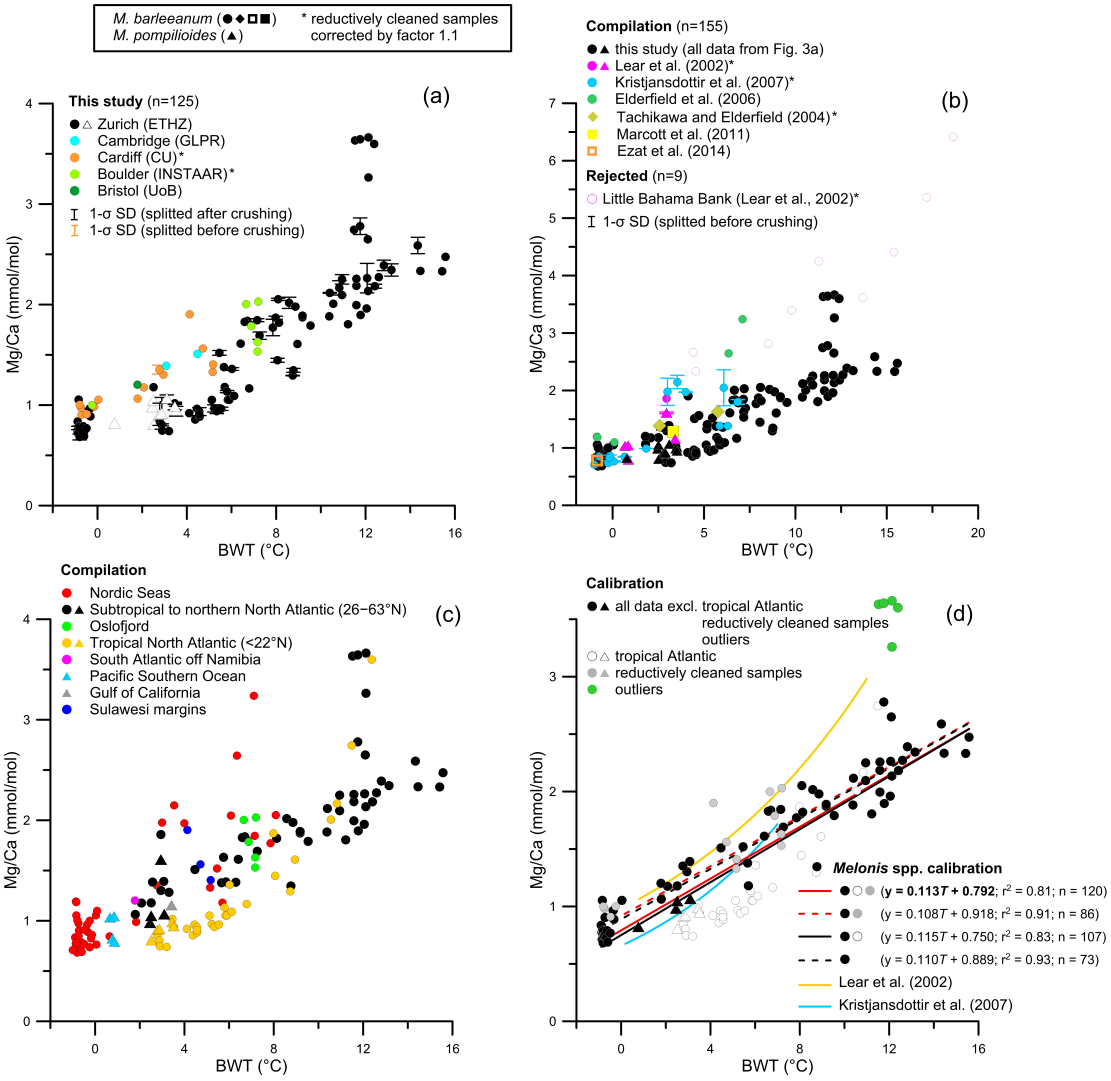

Figure 4. Relationship between bottom water temperature (°C; BWT) and Mg/Ca ratio of *Melonis* (mmol/mol). *Melonis pompilioides* are shown as triangles throughout. Reductively cleaned samples are corrected by factor 1.10 (Yu et al., 2007). (a) Mg/Ca analyses from this study. The SD of the samples processed at CU (orange) and ETHZ (black) include samples, which were split before and after crushing, respectively. (b) Compilation of new and published *Melonis* Mg/Ca ratios. The previously published data from the Little Bahama Bank (Lear et al., 2002) were rejected (open pink circles). (c) Mg/Ca data shown in (b) plotted with the color code labeling the different oceanic regions. (d) Mg/Ca data shown in (a), and differentiating between the tropical Atlantic and all other data, as well as on the cleaning method. The calibration curves only include data newly presented in this study. They are based on the entire data set (red solid line), and on all data excluding the tropical Atlantic data

878 (red dashed line), excluding the reductively cleaned samples (black solid line), and excluding
879 both the tropical Atlantic data and reductively cleaned samples (black dashed line). Also
880 shown are the five outliers in green, and the previously published calibration curves, not
881 corrected for the cleaning method (Lear et al., 2002; Kristjansdottir et al., 2007).

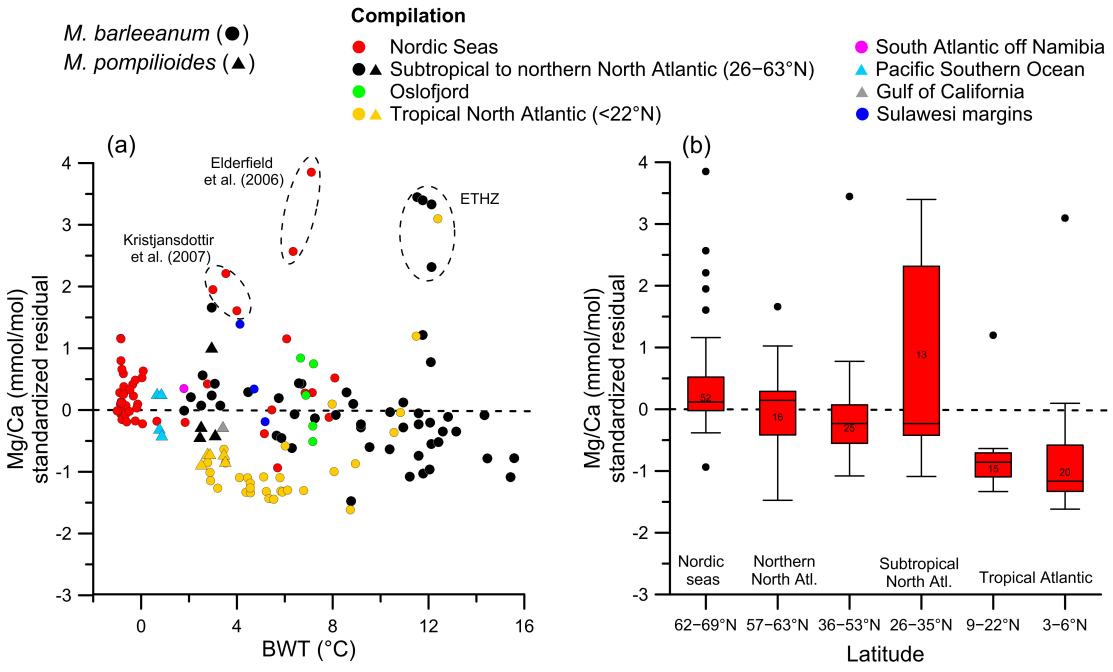

882

883 **Figure 5.** (a) Standardized Mg/Ca residuals of all data shown in Fig. 3b (except for LBB),
884 calculated by removing the temperature trend. (b) Mg/Ca residuals of the North Atlantic
885 grouped into six latitudinal regions. The box whisker plots emphasize the discrepancy
886 between the tropical North Atlantic data and the extratropical North Atlantic data.

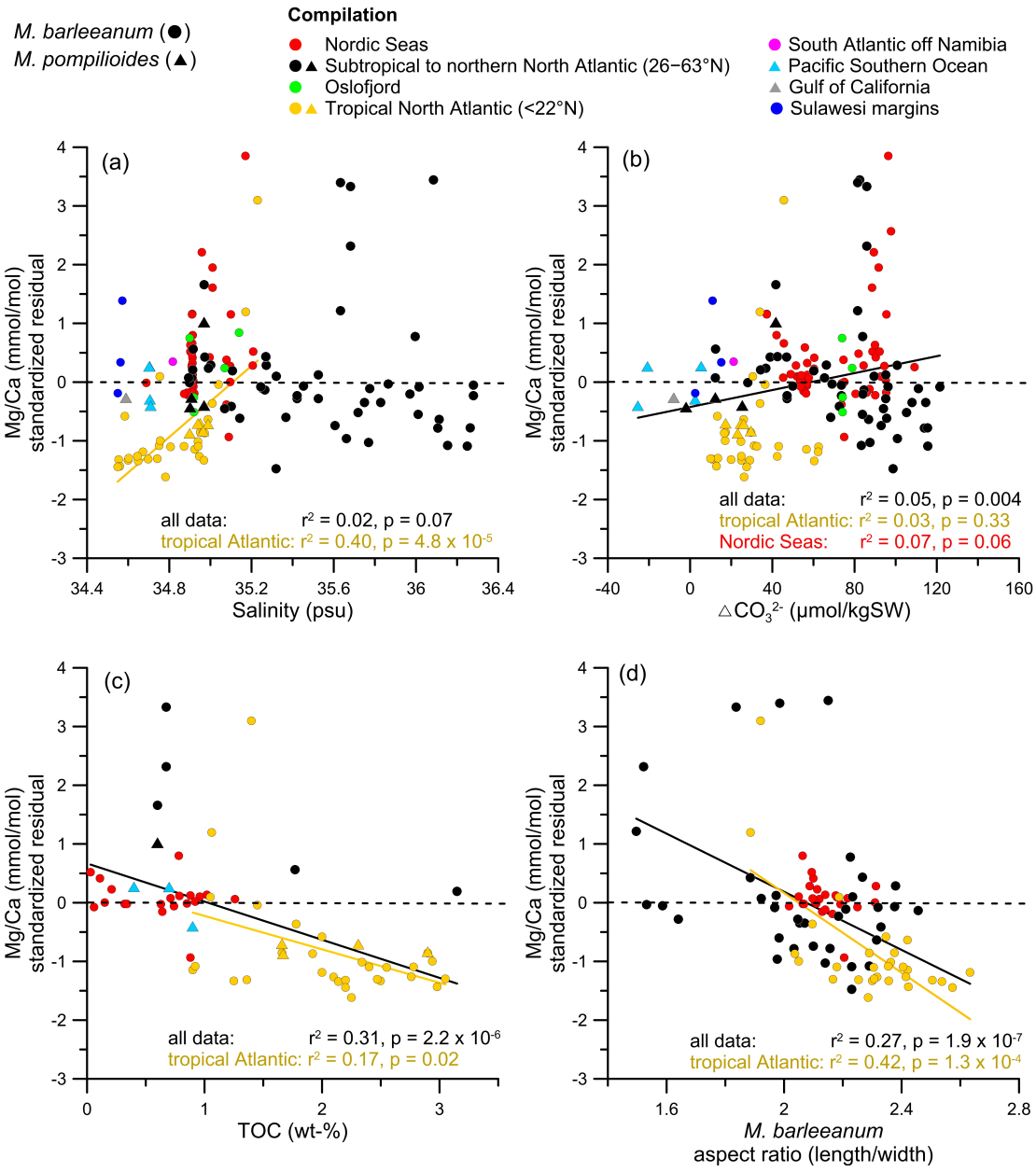

887

888 **Figure 6.** Standardized Mg/Ca residuals compared to (a) salinity, (b) $\Delta[CO_3^{2-}]$, (c) TOC, and

889 (d) the aspect ratio of *M. barleeanum*. The linear fits are only shown when the correlation is

890 significant ($p < 0.05$).